



저작자표시-비영리-변경금지 2.0 대한민국

이용자는 아래의 조건을 따르는 경우에 한하여 자유롭게

- 이 저작물을 복제, 배포, 전송, 전시, 공연 및 방송할 수 있습니다.

다음과 같은 조건을 따라야 합니다:



저작자표시. 귀하는 원저작자를 표시하여야 합니다.



비영리. 귀하는 이 저작물을 영리 목적으로 이용할 수 없습니다.



변경금지. 귀하는 이 저작물을 개작, 변형 또는 가공할 수 없습니다.

- 귀하는, 이 저작물의 재이용이나 배포의 경우, 이 저작물에 적용된 이용허락조건을 명확하게 나타내어야 합니다.
- 저작권자로부터 별도의 허가를 받으면 이러한 조건들은 적용되지 않습니다.

저작권법에 따른 이용자의 권리는 위의 내용에 의하여 영향을 받지 않습니다.

이것은 [이용허락규약\(Legal Code\)](#)을 이해하기 쉽게 요약한 것입니다.

[Disclaimer](#)

Master's Thesis

Design of High Density Spent Fuel Storage Rack
Applying Burnup Credit

Sanggeol Jeong

Department of Nuclear Engineering

Graduate School of UNIST

2018

Design of High Density Spent Fuel Storage Rack Applying Burnup Credit

Sanggeol Jeong

Department of Nuclear Engineering

Graduate School of UNIST

Design of High Density Spent Fuel Storage Rack

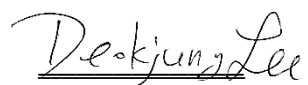
Applying Burnup Credit

A thesis
submitted to the Graduate School of UNIST
in partial fulfillment of the
requirements for the degree of
Master of Science

Sanggeol Jeong

06. 14. 2018

Approved by



Advisor

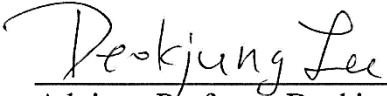
Deokjung Lee

Design of High Density Spent Fuel Storage Rack Applying Burnup Credit

Sanggeol Jeong

This certifies that the thesis of Sanggeol Jeong is approved.

06. 14. 2018



Advisor: Professor Deokjung Lee



Thesis Committee Member: Professor Hyun Chul Lee



Thesis Committee Member: Professor Eisung Yoon

Abstract

Until now, spent nuclear fuel has been evaluated conservatively by assuming the spent nuclear fuel as a fresh fuel in most nuclear fuel criticality safety analysis. However, during irradiation of nuclear fuel in the reactor, fissile materials in nuclear fuel are depleted for power generation. The spent nuclear fuel contains actinides and fission products with large neutron absorption cross-sections, and assuming the spent nuclear fuel as a new fuel has an unnecessary safety margin and increases the spent nuclear fuel storage cost. Taking credit for the reduced reactivity of spent nuclear fuel in criticality safety analyses on spent nuclear fuel handling facilities is referred to as burnup credit. In this study, the design of high density spent fuel storage rack is proposed by using annular cylinder shape of neutron absorber instead of plate type and applying the burnup credit. Through installation of dense rack, the spent fuel storage capacity can be increased.

Contents

I. Introduction.....	1
II. Analysis Methodology	2
2.1. Computer Code.....	2
2.2. Calculation Model	2
2.2.1. Fuel assembly	2
2.2.2. Modeling Assumption.....	2
2.2.3. Description of wet spent fuel storage.....	4
2.2.4. Region I	4
2.2.5. Region II	5
2.2.6. Modeling Assumption.....	5
III. Criticality Analysis	8
3.1. Calculation information.....	8
3.2. Nuclide for burnup credit	8
3.2.1. Regulatory requirement	9
3.3. Results	12
3.3.1. Fuel Assembly Depletion.....	12
3.3.2. Spent fuel pool criticality analysis.....	13
IV. Loading curve	16
V. Sensitivity Analysis	19
5.1. Calculation information.....	19
5.2. Region I	19
5.2.1. Absorber thickness.....	19
5.2.2. Absorber material and concentration.....	20
5.2.3. Rack Pitch.....	23
5.3. Region II.....	23
5.3.1. Absorber thickness.....	23

5.3.2. Absorber material and concentration.....	28
5.3.3. Rack Pitch.....	30
VI. Conclusion	33

List of Figures

Figure 1. YZ and XY geometry of depletion calculational model.	3
Figure 2. Spent fuel storage cell geometry of region I with MCS (Above) and MCNP6 (Below).	6
Figure 3. Spent fuel storage cell geometry of region II with MCS (Above) and MCNP6 (Below).	7
Figure 4. Neutron multiplication factor for different initial enrichment as function of burnup.	13
Figure 5. Neutron multiplication factor for region I and II as function of initial enrichment. Error bars represent 1σ statistical uncertainties.	14
Figure 6. Minimum burnup level for satisfying criticality safety regulatory requirement for conventional design of region II rack	16
Figure 7. Minimum burnup level for satisfying criticality safety regulatory requirement for proposed high density rack design of region II	17
Figure 8. Loading curve for conventional rack.	18
Figure 9. Loading curve for proposed dense rack.	18
Figure 10. Neutron multiplication factor as function of thickness of annular cylinder type of neutron absorber for region I	20
Figure 11. Neutron absorption cross section of ^{10}B and ^{157}Gd as neutron absorber material.	21
Figure 12. Neutron absorption cross section of selected candidates for neutron absorber material.	22
Figure 13. Neutron multiplication factor as function of neutron absorber concentration of boron and gadolinium for region I	22
Figure 14. Neutron multiplication factor as function of concentration of neutron absorber material candidates for region I	23
Figure 15. Neutron multiplication factor as function of rack pitch for region I	24
Figure 16. Neutron multiplication factor as function of thickness of annular cylinder type of neutron absorber for region II	25
Figure 17. Normalized neutron multiplication factor as function of thickness of neutron absorber.	25
Figure 18. Neutron spectrum of guide tube region (thickness of neutron absorber =0.603cm).	26
Figure 19. Neutron spectrum of guide tube region (thickness of neutron absorber =0.843cm).	27
Figure 20. Neutron spectrum of inner water region at guide tube.	27
Figure 21. Neutron multiplication factor as function of neutron absorber concentration of boron and gadolinium for region II	29
Figure 22. Neutron multiplication factor as function of concentration of neutron absorber material candidates for region II	29
Figure 23. Neutron multiplication factor as function of rack pitch for region II.	30
Figure 24. Conventional (Above) and proposed (Below) design of region I	31
Figure 25. Conventional (Above) and proposed (Below) design of region II.	32

List of Tables

Table 1. 16 x 16 Fuel Assembly characteristics for depletion calculation model	4
Table 2. Nuclides used in applying burnup credit criticality analysis.....	9
Table 3. Physical Parameters for Areas of Applicability.....	11
Table 4. Nuclides used in applying burnup credit criticality analysis.....	11
Table 5. Nuclides used in applying burnup credit criticality analysis.....	12
Table 6. Multiplication factor as a function of initial enrichment.....	14
Table 7. Multiplication factor of region I and II with 1.72 wt% initial enrichments	15
Table 8. Minimum burnup of region II as a function of initial enrichment	17

I. Introduction

The spent nuclear fuel is stored in the water pools in the nuclear power plant. In the Republic of Korea, it is expected that the temporary storage facilities in Wolsong and Hanbit nuclear power plants will be saturated by 2019 and 2024, respectively. The intermediate storage facility will be completed only by 2035 [1]. Hence, according to the spent fuel management plan, it is necessary to secure additional temporary storage facilities on the site by that time. As an alternative, storage capacity can be increased by replacing or re-racking of existing spent fuel storage to high density spent fuel storage. The high density spent nuclear fuel storage contains more fuel elements due to the reduced space between assemblies. However, as more spent fuel is inserted into a space of equal size, the criticality increases. The criticality safety of spent nuclear fuel should be maintained at the same level. To reduce the spacing between fuel assemblies, placing the annular cylinder type of neutron absorber into the water holes of assemblies, changing the type and concentration of the material used in the neutron absorber are proposed in this research.

Until now, the spent nuclear fuel has been evaluated conservatively by assuming the spent nuclear fuel as a fresh fuel in the most nuclear fuel criticality safety analysis. However, the spent nuclear fuel contains fission products with a large neutron absorption cross sections. Therefore, the criticality should be evaluated in consideration of this fact. Hence, the burnup credit is applied considering the irradiation of the spent fuel. The methodology beyond the burnup credit [2-8] and benefits from its application in the criticality safety analysis [9] are studied. The criticality calculations are performed using two continuous energy Monte Carlo (MC) neutron transport codes MCNP6 [10] developed in Los Alamos National laboratory, and MCS [11] developed in COmputational Reactor physics and Experiment laboratory (CORE) in the Ulsan National Institute of Science and Technology (UNIST). Both MC codes utilize the ENDF/B-VII.1 [12] nuclear cross section data library.

II. Analysis Methodology

2.1. Computer Code

The MCS, used for the criticality and depletion calculations in this study, is an in-house 3D continuous-energy neutron-physics code for performing particle transport calculations based on the Monte Carlo method. It uses the continuous energy neutron cross section library ENDF/B VII.1. It is possible to perform criticality run for reactivity calculations and fixed-source run for shielding problems using MCS code. It is developed with the purpose of solving complex multi-physics full core problems such as the BEAVRS core (Benchmark for Evaluation And Validation of Reactor Simulation) [13] with high accuracy and high performance, using internal universe and lattice functions to model the 3D geometry. Its continuous-energy analysis capability has been verified and validated against various benchmarks: BEAVRS, H-M (Hoogenboom-Martin) [14], VENUS-2 [15].

2.2. Calculation Model

2.2.1. Fuel assembly

In this study, a fuel assembly of APR-1400 reactor was chosen for depletion calculation using MCS. The selected APR-1400 reactor fuel assembly is composed of a 16 x 16 array of fuel rods, guide tubes and instrumentation tube. Each fuel assembly has 236 fuel pins as shown in Figure 1, and the fuel material is uranium dioxide (UO₂) surrounded by thin-walled zircaloy cladding. The fuel pin pitch is 1.285 cm, and outer radius of cladding is 0.4750 cm. The fuel temperature is 900 K, and the other regions are at 600 K. The detailed information about the geometry of assembly is described in Table 1. The maximum initial enrichment of the fuel is 4.50 w/o ²³⁵U, and the fuels are depleted up to 60 MWd/kgU burnup.

2.2.2. Modeling Assumption

To improve the computational efficiency in this study, the calculations were performed without simulating structures that did not affect the criticality. The calculation model of fuel assembly is developed with the following assumptions through MCS computer code.

- a. The computational model for fuel assembly has a reflective boundary condition in X and Y directions and thus the developed model has an infinite array.
- b. All fuel assemblies used in the depletion calculation model consist of one type with the same

- initial enrichment (UO_2 fuel rods) and nuclear fuel rod arrangement.
- c. The calculation model assumes 30 cm of water is filled above and below the active fuel zone.
 - d. The fuel density of UO_2 is 10.313 g/cm^3 ;
 - e. The spacer grids and other structural material are replaced with water.
 - f. The modeling doesn't contain any burnable poisons or control rod.
 - g. The 900K and 600K cross section libraries were used in the MC simulations.

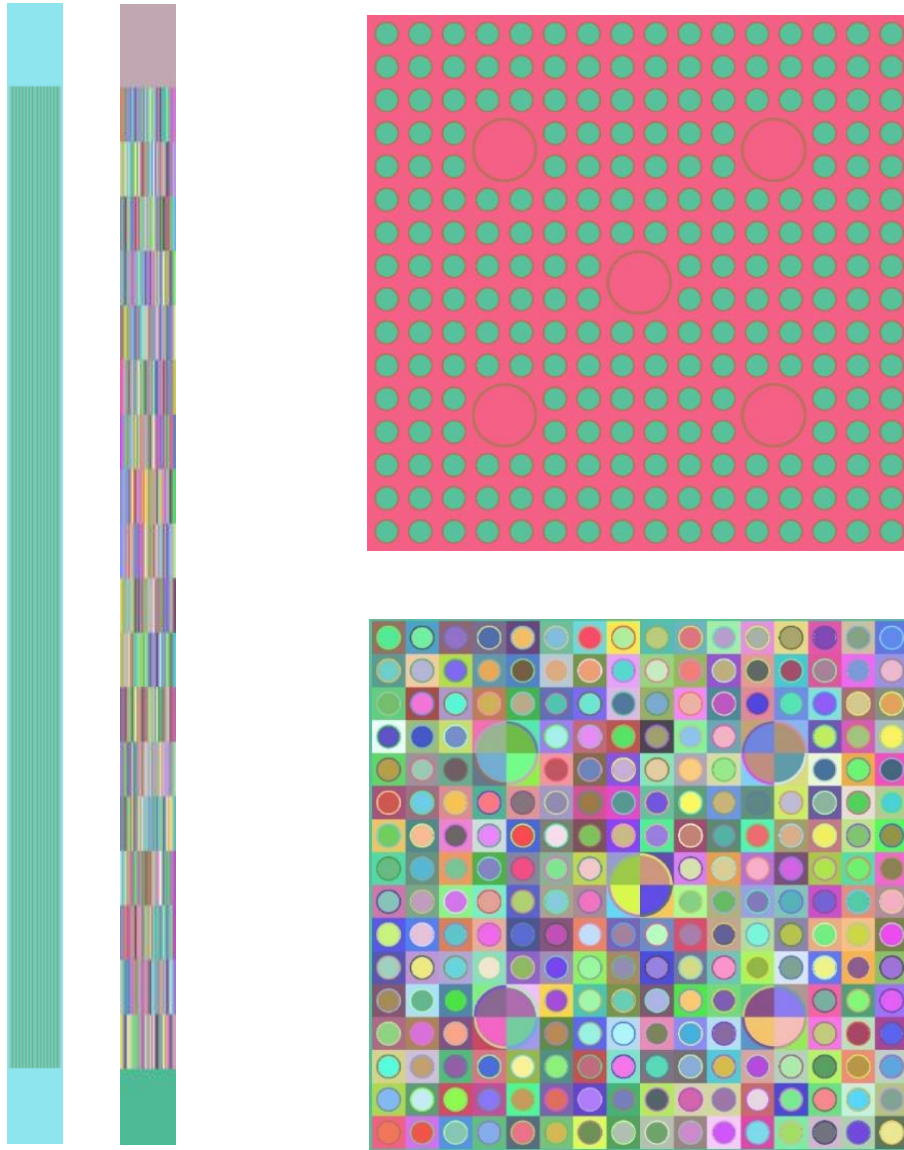


Figure 1. YZ and XY geometry of depletion calculational model.

Table 1. 16 x 16 Fuel Assembly characteristics for depletion calculation model

Description	
# of fuel rods	236
Rod pitch (cm)	1.285
Assembly width (cm)	20.774
Active fuel length (cm)	383.3262
Enrichment (²³⁵ U wt.%)	1.72
Fuel pellet, O.D. (cm)	0.4095
Cladding, O.D. (cm)	0.4750
Cladding, I.D (cm)	0.4180
Instrument tube, O.D (cm)	1.1430
Instrument tube, I.D (cm)	1.2445

2.2.3. Description of wet spent fuel storage

The main function of the spent fuel storage facilities is to safely store the fresh and spent fuel assemblies in a water tank. The criticality of the spent fuel pool is controlled by the rack design of spent fuel storage; it is dependent on the spacing between fuel assemblies, the thickness and the composition of the neutron absorbers.

There are two regions in the spent fuel storage pool. A region I is designed for storing fresh (not irradiated) fuel, and the region II is used for irradiated fuel. It is important to note that Region I and II have different designs, former requires insertion of two neutron absorber plates between assemblies, and latter region – only one.

2.2.4. Region I

The region I storage cells are composed of stainless steel grids with the water flux trap to control reactivity between two plates of neutron absorber. Figure 2 shows the configuration of the conventional design (CD) of rack for region I modeled using MCS and MCNP6. The single storage cell region I is isolated by the stainless-steel wall. The pitch of the region I storage cell is 27.00 cm. The role of stainless steel structure is to support nuclear fuel assemblies and plate type of neutron absorbers located between storage cells. The plate type of neutron absorber has a thickness of 0.25 cm, a width of 18 cm and a height of 383.3262 cm, which is equal to the height of active fuel. The neutron absorber is located on

four sides of the stainless-steel wall in relation to the fuel assembly. The proposed geometry of region I spent fuel pool is shown in Figure 18. Region I, which stores fresh fuel, is not subject of reactivity reduction, unlike region II. Therefore, both plate-type neutron absorbers and the suggested annular cylinder type of neutron absorbers are used to control the increase in reactivity due to dense rack installation. The plate type of neutron absorber uses the same design as the conventional one, and the dense rack is designed by reducing the space of the flux trap located between the storage cells outside of the plate type neutron absorber.

2.2.5. Region II

The fresh fuel is stored into Region I, while in the region II is used for irradiated fuel. Region II is designed for the storage of fuel which has accumulated a minimum burnup based on initial enrichment. Figure 3 shows the configuration of the conventional design of rack for region II developed with MCS and MCNP6. Like Region I, each storage cell is divided by a stainless-steel wall, and a plate type of neutron absorber is attached to the side wall of the stainless steel structural wall. Unlike Region I, where two neutron absorber plates are located between storage cells, Region II uses one neutron absorber plate between storage cells and the size of the storage rack is 22.60 cm. The plate-type neutron absorber has a thickness of 0.42, a width of 19.4 and a height of 383.3262. The structure of the proposed Region II is shown in figure 25. The proposed annular cylinder type of neutron absorber is used to reduce the reactivity instead of plate type of neutron absorber. A dense rack was designed by reducing the space of the water gap located outside the nuclear fuel assembly and the area where the neutron absorber plate was located.

2.2.6. Modeling Assumption

To improve the computational efficiency in this study, the calculations were performed without simulating structures that did not affect the criticality. The MCS and MCNP calculation model of fuel assembly is developed with following assumptions.

- a. The computational model for fuel assembly has a reflective boundary condition in the X and Y directions and thus developed model has an infinite array.
- b. The geometry of fuel assembly inserted to spent fuel storage is same with the model of section 2.2.1. The structural materials such as the plenum and spring end cap of the fuel rod and areas beyond the active fuel length are assumed to be ignored and replaced by water.
- c. It is assumed that the fuel assembly, the rack structure, and water are at room temperature.

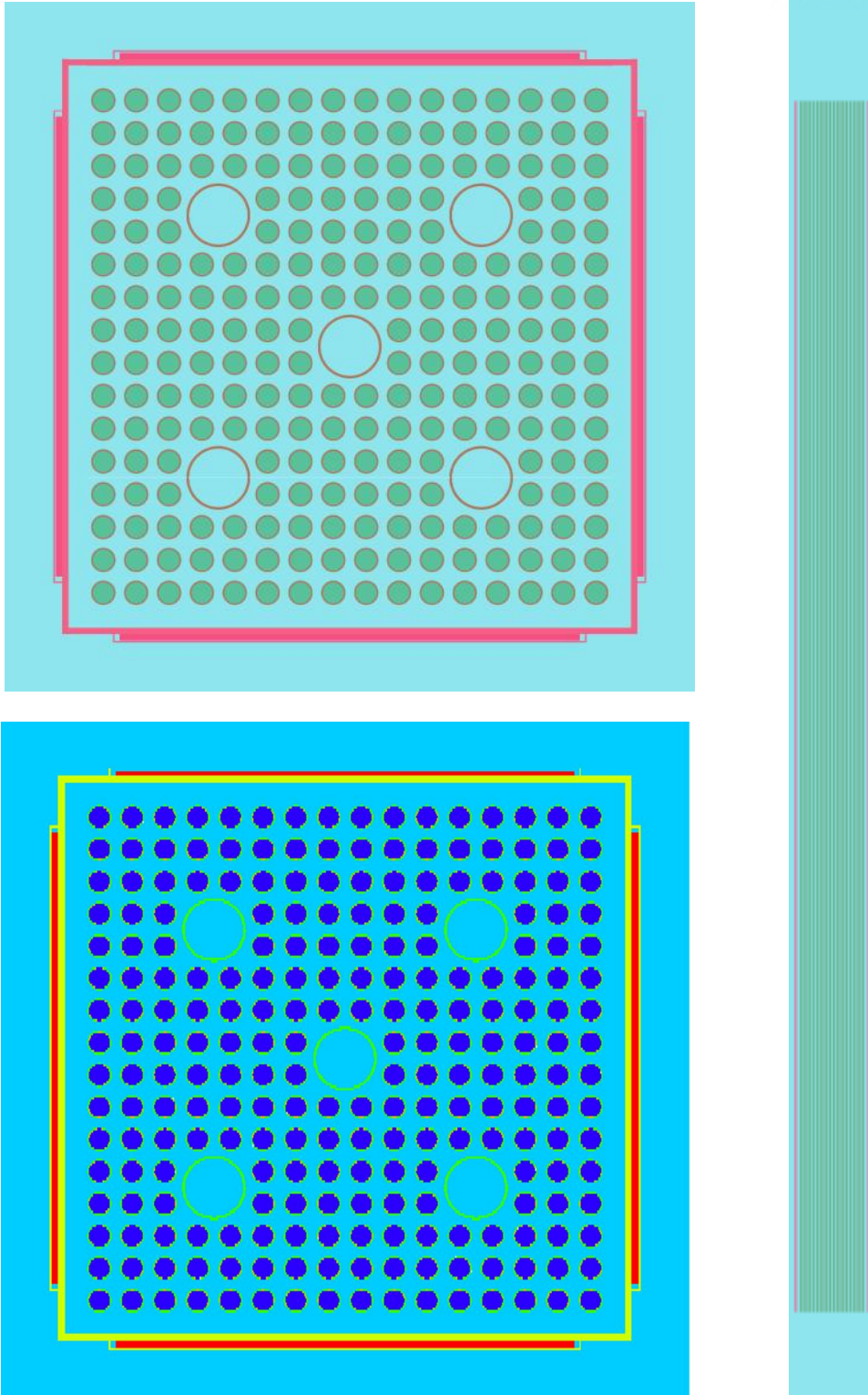


Figure 2. Spent fuel storage cell geometry of region I with MCS (Above) and MCNP6 (Below).

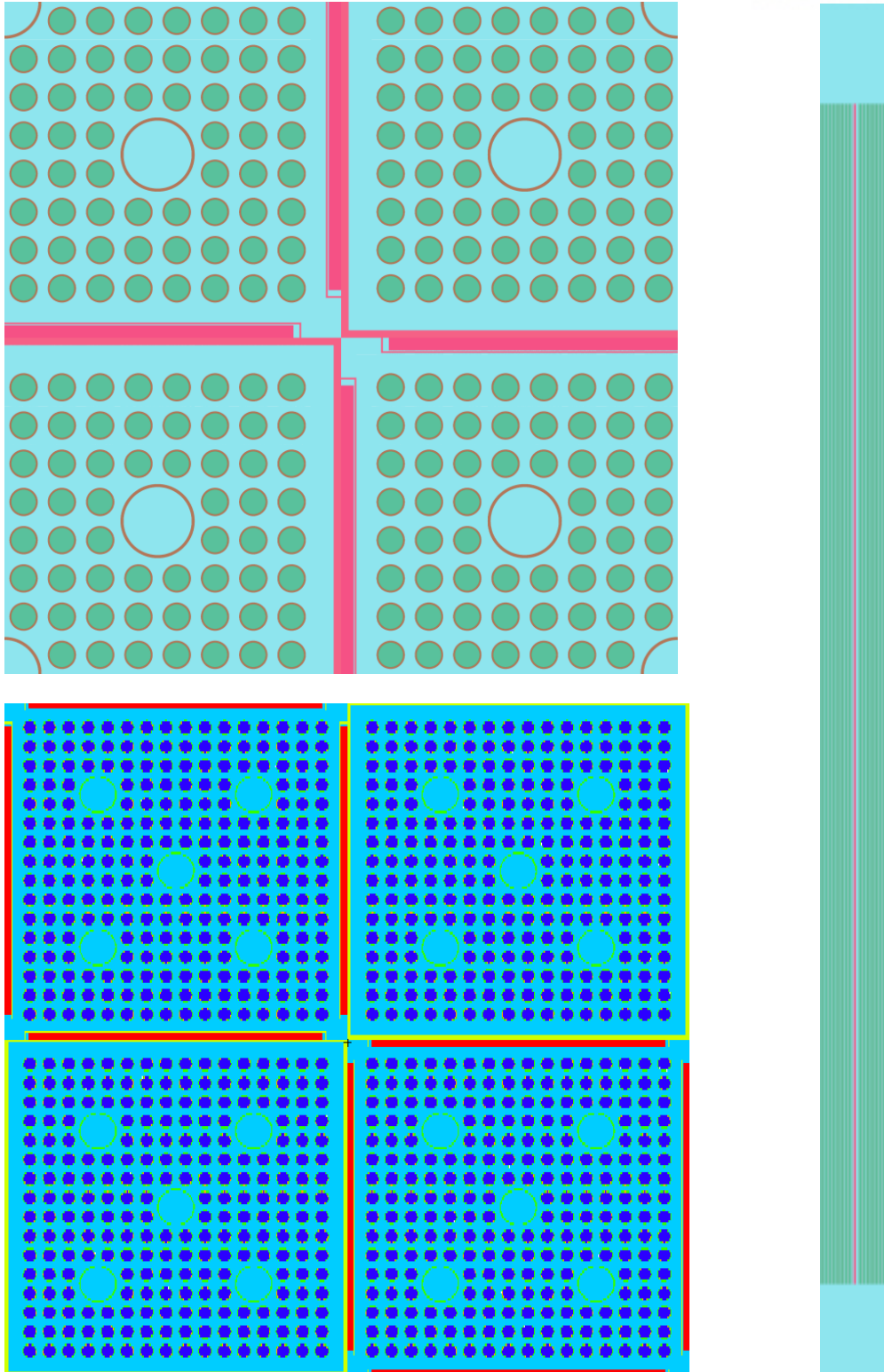


Figure 3. Spent fuel storage cell geometry of region II with MCS (Above) and MCNP6 (Below).

III. Criticality Analysis

3.1. Calculation information

The depletion calculations are performed using the MCS with ENDF/B-VII.1 continuous energy cross section libraries. As discussed in section 2.2.1, the depletion calculation model is 16 x 16 PLUS7 fuel assembly, used in Shin Kori Unit 3 (APR-1400). The multiplication factors (k_{eff}) and isotopic concentrations are generated at each burnup step from 0 to 60 MWd/kgU. The depletion calculation is performed with 16 different initial enrichments: 1.72, 2.00, 2.30, 2.40, 2.57, 2.65, 2.80, 2.90, 3.00, 3.05, 3.10, 3.14, 3.19, 3.50, 3.64 and 4.50 wt% ^{235}U . In case of the 1.72 and 2.50 wt% ^{235}U initial enrichments, 48 burnup steps from 0 to 40 MWd/kgU are used in depletion calculations. The other initial enrichments cases are calculated using 64 burnup steps up to 60 MWd/kgU. The irradiation is continuous with a specific power density of 33 W/gU. For simplicity, the depletion calculations were performed with temperatures of 900 K for the nuclear fuel and 600 K for the other materials. The three-dimensional (3D) calculations with a reflective boundary condition for X, Y directions, and black boundary condition for Z direction were performed for all cases with calculated axial burnup profiles. As described in Figure 1, the fuel pins are divided into 18 axial burnable zone [16], and the specific power distribution is calculated with Monte Carlo simulation. As the results, the isotopic concentrations are calculated for each fuel pin and each axial zone. These calculated nuclide compositions are used to analyze criticality of the region II in the spent fuel pool. The Monte Carlo simulations used 5 active, 5 inactive cycles with 30 multicycles, and 100,000 neutrons per cycle. The standard deviations of the multiplication factors range approximately from 5 pcm to 35 pcm. For the criticality calculation of region I and II in the spent fuel storage, the MCS criticality analyses were performed using 100,000 neutron histories per cycle, 10 inactive, 10 active cycles and 20 multicycles. The standard deviations of the multiplication factors range approximately from 13 pcm to 16 pcm.

3.2. Nuclide for burnup credit

The fuel compositions for these models consist of 28 actinides and fission products that are important to fuel reactivity (i.e., nuclides with large neutron fission cross sections and large neutron absorption cross sections). In the criticality safety analysis of spent fuel considering the burnup of nuclear fuel, it is necessary to take into account the reduction of the fissile material due to the nuclear fission during the operation, production and decay of the actinides and the fission products in the fuel. In comparison to the fresh fuel, there are some nuclides in the composition of the spent fuel that can lead to a change in the reactivity. ^{235}U , ^{239}Pu and ^{241}Pu in the spent fuel are the nuclides that have positive

reactivity, and other nuclides that bring negative reactivity can be generated as a result of decay of ^{241}Pu to ^{241}Am and the formation of ^{155}Gd from the beta decay of ^{155}Eu . The nuclides considered for burnup credit are divided into three groups based on the importance to fuel reactivity. As shown in Table 5, twelve actinide and sixteen fission product isotopes are selected from NUREG/CR-7109 [8], the document of Nuclear Regulatory Commission (NRC), and the 28 nuclides are ^{234}U , ^{235}U , ^{236}U , ^{238}U , ^{237}Np , ^{238}Pu , ^{239}Pu , ^{240}Pu , ^{241}Pu , ^{242}Pu , ^{241}Am , ^{243}Am , ^{95}Mo , ^{99}Tc , ^{101}Ru , ^{103}Rh , ^{109}Ag , ^{133}Cs , ^{143}Nd , ^{145}Nd , ^{147}Sm , ^{149}Sm , ^{150}Sm , ^{151}Sm , ^{152}Sm , ^{151}Eu , ^{153}Eu and ^{155}Gd . The selected nuclides are divided to three groups.

- a. Actinides only
- b. Actinides and sixteen fission products
- c. Actinides and all fission products

Table 2. Nuclides used in applying burnup credit criticality analysis

Set of nuclides for actinide-only burnup credit (12)			
^{234}U	^{235}U	^{236}U	^{238}U
^{237}Np	^{238}Pu	^{239}Pu	^{240}Pu
^{241}Pu	^{242}Pu	^{241}Am	^{243}Am
Set of nuclides for actinides and fission product (16)			
^{95}Mo	^{99}Tc	^{101}Ru	^{103}Rh
^{109}Ag	^{133}Cs	^{143}Nd	^{145}Nd
^{147}Sm	^{149}Sm	^{150}Sm	^{151}Sm
^{152}Sm	^{151}Eu	^{153}Eu	^{155}Gd

3.2.1. Regulatory requirement

According to the licensing criteria, the sub-criticality of the spent fuel storage pool is guaranteed when the maximum k_{eff} value of system is less than 0.95 including the uncertainties at a 95 percent probability, 95 percent confidence level. This uncertainty consists of a statistical combination, the maximum k_{eff} being expressed as in Eq. (1).

$$k_{eff}^{max} = 1.0 + Bias - \Delta\sigma_{Bias} - \Delta_{SM} - \Delta_{AOA}, (1)$$

The document, 10 CFR 50.68, “Criticality Accident Requirements,” [17] states: “If no credit for soluble boron is taken, the k-effective of the spent fuel storage racks loaded with fuel of the maximum fuel assembly reactivity must not exceed 0.95, at a 95 percent probability, 95 percent confidence level, if flooded with unborated water. If credit is taken for soluble boron, the k-effective of the spent fuel storage racks loaded with fuel of the maximum fuel assembly reactivity must not exceed 0.95, at a 95 percent probability, 95 percent confidence level, if flooded with borated water, and the k-effective must remain below 1.0 (subcritical), at a 95 percent probability, 95 percent confidence level, if flooded with unborated water.”

The above value known as upper safety limit (USL, hereinafter referred to as "USL1" are used to assure sub-criticality of systems. In addition, another criticality safety standard is obtained as the upper safety limit [18-19] (USL, hereinafter referred to as "USL2") by the methodology presented in the technical documentation of the United States Nuclear Regulatory Commission (U.S.NRC), “Guide for Validation of Nuclear Criticality Safety Calculational Methodology (NUREG/CR-6698)” [20]. Statistical analysis is performed in accordance with the proposed methodology of the documents to determine the statistical significance of the input data used as the criticality safety benchmark experiments. The target for the criticality safety analysis is the nuclear fuel storage facility for the light water reactor, and the selected criticality benchmark experiments shall reflect the characteristics of the target for which the actual criticality safety is to be assessed. The 279 critical experiments satisfying the areas of applicability as shown in table 3 were selected from the "International Handbook of Evaluated Criticality Safety Benchmark Experiments” published by the International Criticality Safety Benchmark Evaluation Project (ICSBEP) [21], and they are shown in Table 4. The neutron multiplication factors for guaranteeing criticality safety are obtained with USL1 and USL2, these results are shown in Table 5.

Table 3. Physical Parameters for Areas of Applicability

Parameter	Range
Fissionable material	UO ₂
Lattice type	Square
Enrichment (wt% ²³⁵ U)	2.35 to 4.74
H/U	0.4683 to 11.5398
Lattice pin pitch (cm)	1.075 to 2.540
Temperature (K)	289 to 298
Reflector	Water, Lead, Depleted Uranium and Carbon steel
Moderating material	Water

Table 4. Nuclides used in applying burnup credit criticality analysis

Experiments	# of case	Enrichment (wt%)	Fuel Pin Pitch (cm)	H/U
LCT-001	8	2.35	2.032	2.9177
LCT-002	5	4.31	2.540	3.8821
LCT-006	18	2.60	1.849 ~ 2.293	1.5008 ~ 2.9994
LCT-007	4	4.74	1.260 ~ 2.520	1.8231 ~ 11.5398
LCT-008	17	2.46	1.636	1.8410
LCT-009	27	4.31	2.540	3.8821
LCT-010	30	4.31	1.892, 2.540	1.5970, 3.8821
LCT-011	15	2.46	1.636	1.8413
LCT-013	7	4.31	1.892	1.5970
LCT-016	32	2.35	2.032	2.9177

Experiments	# of case	Enrichment (wt%)	Fuel Pin Pitch (cm)	H/U
LCT-017	29	2.35	1.684, 2.032	1.5995, 2.9177
LCT-035	2	2.60	1.956	1.8326
LCT-039	17	4.74	1.260	1.8231
LCT-042	7	2.35	1.684	1.5995
LCT-050	7	4.74	1.300	2.0320
LCT-051	9	2.46	1.636	1.8413
LCT-054	8	4.35	1.500	1.5008
LCT-065	17	2.60	1.956	1.4249
LCT-071	4	4.74	1.075, 1.100	0.4683, 0.5251
LCT-072	3	4.74	1.600	1.9400
LCT-089	4	4.35	1.500	2.6399
LCT-090	9	4.35	1.500	2.6420

Table 5. Nuclides used in applying burnup credit criticality analysis

	USL1	USL2
Multiplication factor	0.95	0.9736 ($1\sigma = 21$ pcm)

3.3. Results

3.3.1. Fuel Assembly Depletion

Figure 4 shows the neutron multiplication factors (k_{eff}) calculated by MCS for the infinite fuel assembly problem. The APR1400 fuel assembly with 16 x 16 lattice of the fuel pin that included 5 guide tubes filled with water. The initial enrichments of UO₂ fuel are 1.72, 2.00, 2.30, 2.40, 2.57, 2.65, 2.80, 2.90, 3.00, 3.05, 3.10, 3.14, 3.19, 3.50, 3.64 and 4.50 235U in weight. The fuel assemblies are depleted

up to 40 MWd/kgU for 1.72, 2.00 wt% initial enrichments, and 60 MWd/kgU for the others cases. The multiplication factors for initial burnup step are 1.07575, 1.12145, 1.16048, 1.17253, 1.19020, 1.19849, 1.21253, 1.22150, 1.22941, 1.23355, 1.23701, 1.24057, 1.24401, 1.26580, 1.27422 and 1.31793 for all initial enrichments, respectively. The error bars represent 1σ statistical uncertainty.

3.3.2. Spent fuel pool criticality analysis

Table 3 shows the neutron multiplication factors (k_{eff}) of the regions I and II calculated by MCS and MCNP6 for fresh and depleted fuel compositions. The k_{eff} differences are 37 and 50 pcm for the regions I and II, respectively. Figure 5 shows the multiplication factors calculated by MCS for the regions I and II. In case of the region II, the neutron multiplication factors are calculated with four nuclide composition groups, including the fresh fuel composition as described in the Section 3.2. The k_{eff} difference between the fresh and 60 MWd/kgU depleted fuel with 3.14 wt% initial enrichments is 8099 pcm and the k_{eff} values are 1.03616, 0.95517, 0.97595 and 0.96175 for four nuclide inventories (fresh fuel, depleted fuel with all nuclide, twelve actinides and 28 nuclides), respectively. In Figure 5, the multiplication factors for 1.72 and 2.00 wt% initial enrichments are calculated with the 40 MWd/kgU depleted fuel composition exceptionally.

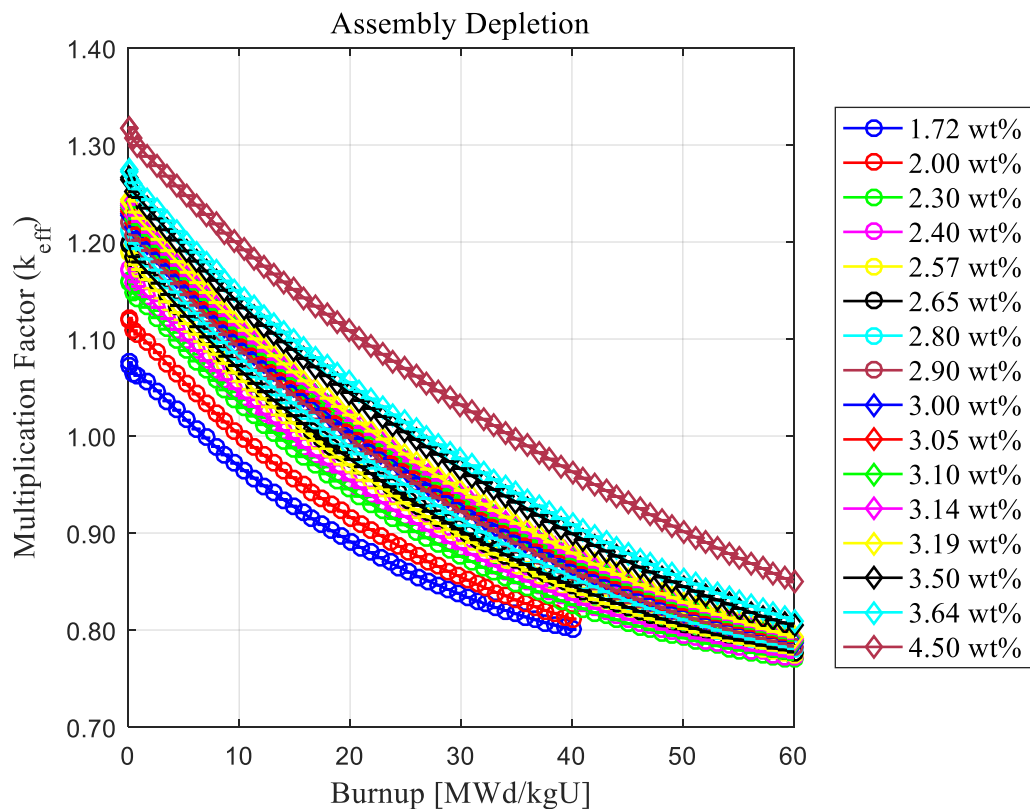


Figure 4. Neutron multiplication factor for different initial enrichment as function of burnup.

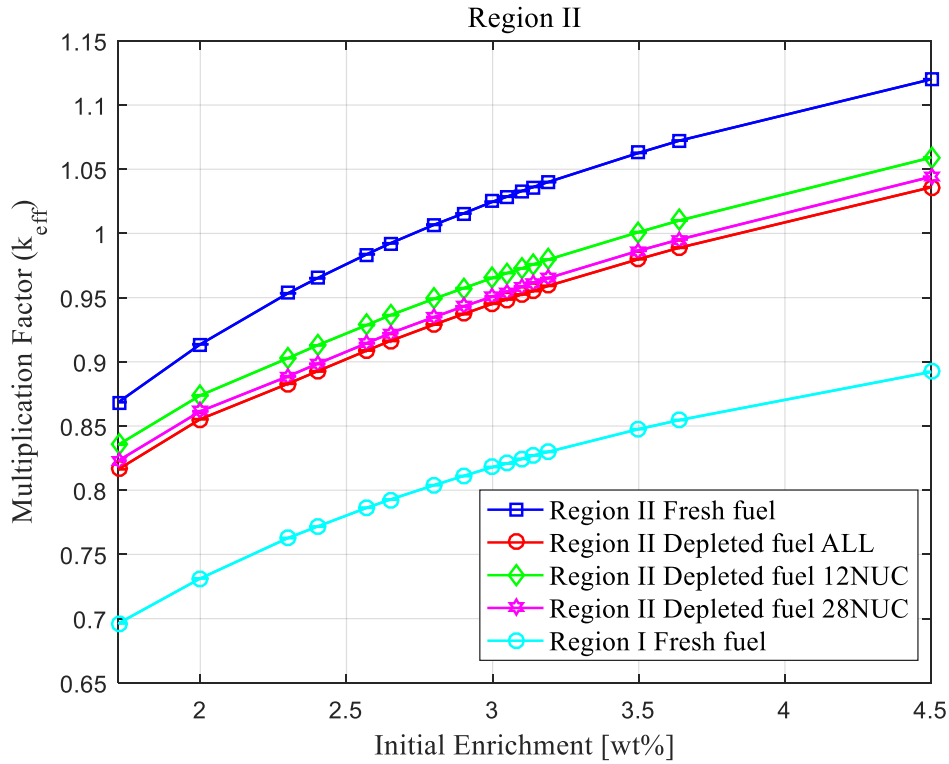


Figure 5. Neutron multiplication factor for region I and II as function of initial enrichment. Error bars represent 1σ statistical uncertainties.

Table 6. Multiplication factor as a function of initial enrichment

Initial Enrichment (w/o)	k_{eff} (Region II, Fresh fuel)	1σ	k_{eff} (Region I, Fresh fuel)	1σ
1.72	0.86861	0.00016	0.69630	0.00013
2.00	0.91365	0.00013	0.73131	0.00013
2.30	0.95343	0.00009	0.76278	0.00014
2.40	0.96509	0.00018	0.77167	0.00014
2.57	0.98381	0.00022	0.78635	0.00014
2.65	0.99232	0.00014	0.79275	0.00014
2.80	1.00678	0.00024	0.80395	0.00015
2.90	1.01552	0.00012	0.81106	0.00014
3.00	1.02470	0.00014	0.81807	0.00014
3.05	1.02869	0.00022	0.82081	0.00015
3.10	1.03306	0.00021	0.82439	0.00014
3.14	1.03620	0.00015	0.82713	0.00015

3.19	1.04001	0.00022	0.82989	0.00015
3.50	1.06272	0.00016	0.84764	0.00015
3.64	1.07230	0.00013	0.85468	0.00014
4.50	1.12003	0.00017	0.89213	0.00015
Initial Enrichment (w/o)	k_{eff} (Region II, Depleted Fuel with All nuclides)	1σ	k_{eff} (Region II, Depleted Fuel with 28 nuclides)	1σ
1.72	0.81639	0.00016	0.83553	0.00019
2.00	0.85534	0.00014	0.87387	0.00016
2.30	0.88295	0.00016	0.90284	0.00013
2.40	0.89261	0.00026	0.91283	0.00010
2.57	0.90884	0.00014	0.92864	0.00015
2.65	0.91627	0.00015	0.93633	0.00013
2.80	0.92904	0.00016	0.94912	0.00019
2.90	0.93719	0.00026	0.95729	0.00019
3.00	0.94530	0.00019	0.96540	0.00023
3.05	0.94864	0.00019	0.96915	0.00010
3.10	0.95251	0.00010	0.97277	0.00013
3.14	0.95517	0.00019	0.97595	0.00014
3.19	0.95914	0.00013	0.97963	0.00019
3.50	0.98001	0.00018	1.00101	0.00022
3.64	0.98894	0.00027	1.01014	0.00017
4.50	1.03594	0.00020	1.05907	0.00021

Table 7. Multiplication factor of region I and II with 1.72 wt% initial enrichments

Multiplication factor	Region I	Region II	1σ (pcm)
MCS (Fresh Fuel)	0.69657	0.86881	11
MCNP6 (Fresh Fuel)	0.69620	0.86831	13
MCS (Depleted Fuel)	-	0.80975	12
Calculation time (min)	86.99 (MCNP6), 41.38 (MCS)	92.58 (MCNP6), 49.38 (MCS)	-

IV. Loading curve

The fuel assembly can be stored in the spent fuel pool, when the multiplication factor of the system is satisfied the regulatory requirement to ensure the subcriticality. In this section, the minimum burnup levels can meet the criticality safety standards are described for the fuel assembly with 16 initial enrichments. Three sets of isotopic compositions discussed in Section III are applied to the inventories of the depleted fuels. The criticality analyses using MCS are performed to obtain the required minimum burnup levels, which satisfy lower k_{eff} than USL1 and USL2. Figures 6-9 illustrate multiplication factor comparison results. In case of the conventional rack of the region II, 0 MWd/kgU burnup is required to be store to region II spent fuel pool for the 1.72, 2.00, 2.30 wt% initial enrichments while the fuel assemblies have higher initial enrichments than 3.10 wt% can't be store to the region II since the multiplication factors of those systems don't stratified the regulatory requirements with 60 MWd/kgU burnup level. If the criticality safety standards of USL2 is applied, the assembly that has 3.19 wt% initial enrichment with the 39.02 MWd/kgU average burnup can be loaded into spent fuel storage.

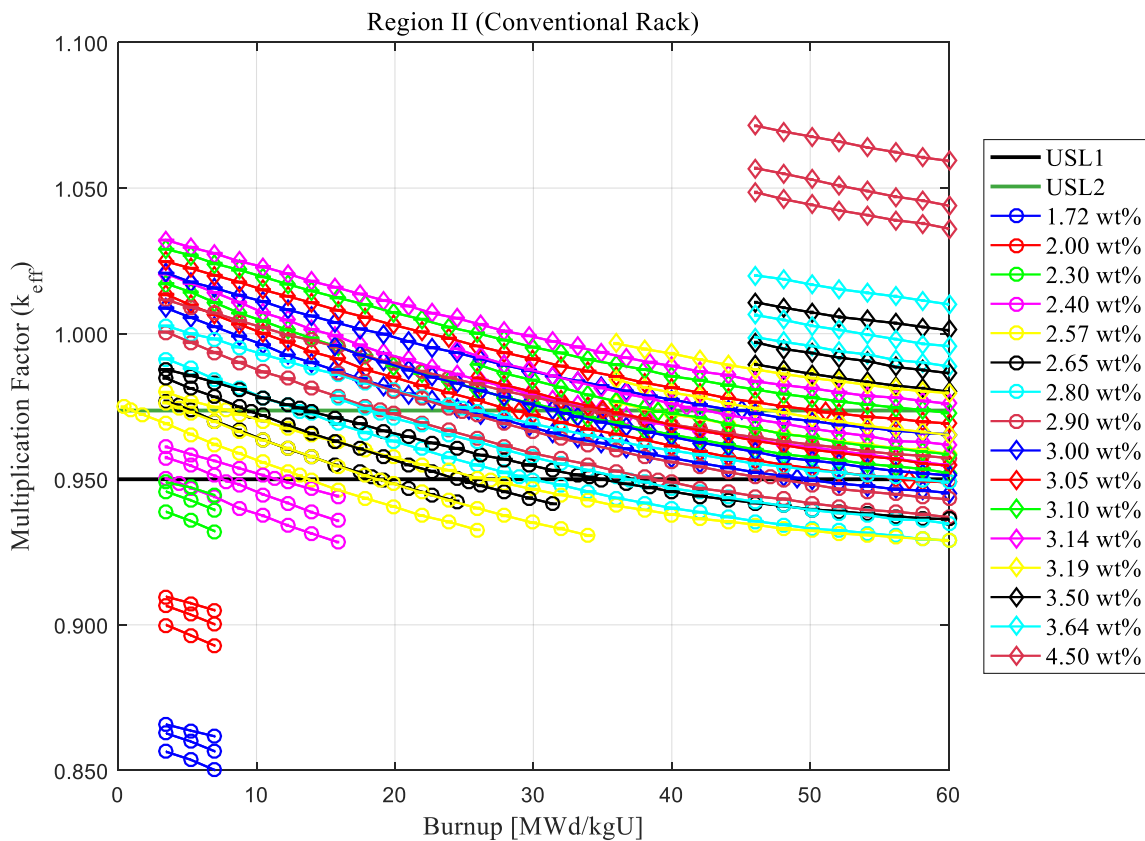


Figure 6. Minimum burnup level for satisfying criticality safety regulatory requirement for conventional design of region II rack

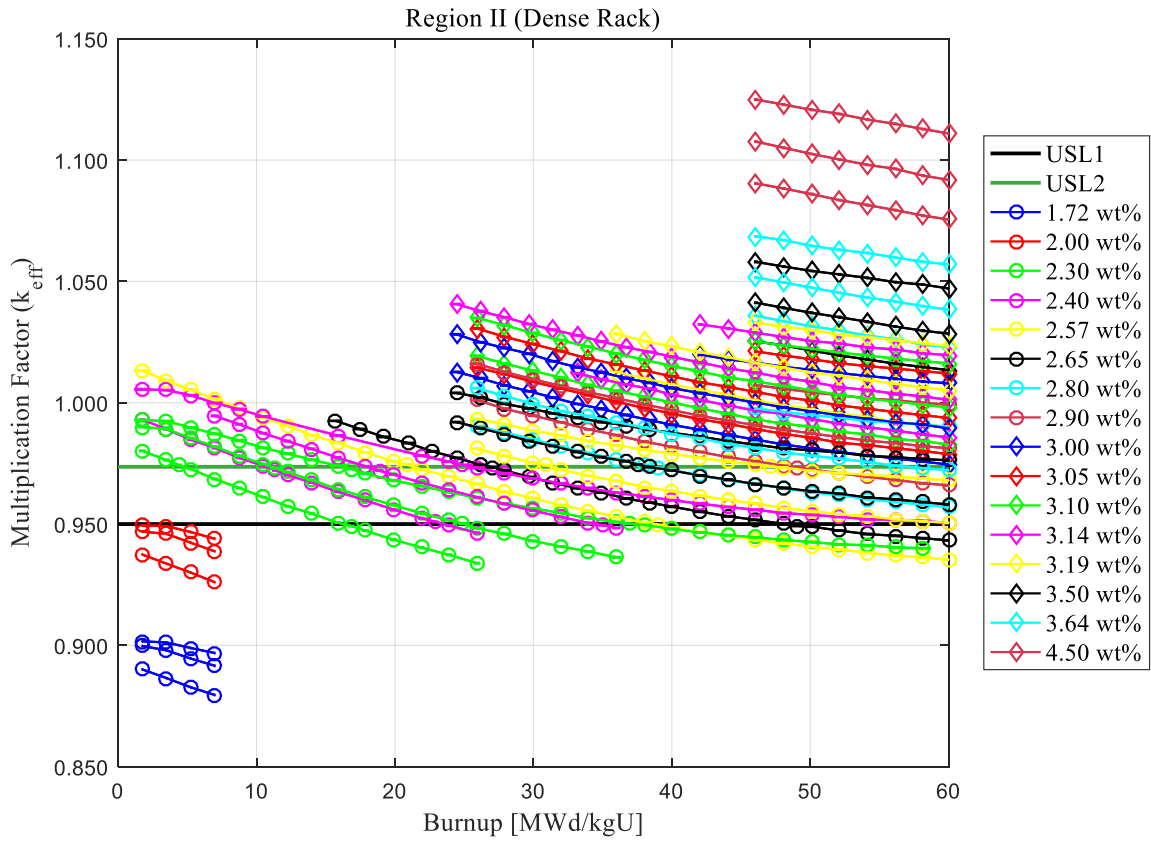


Figure 7. Minimum burnup level for satisfying criticality safety regulatory requirement for proposed high density rack design of region II

Table 8. Minimum burnup of region II as a function of initial enrichment

Initial Enrichment (w/o)	Minimum Burnup for USL1 (MWd/kgU)	Minimum Burnup for USL2 (MWd/kgU)
2.00	-	-
2.4	4.37	-
2.57	13.97	1.75
2.8	29.96	13.10
3	50.11	26.19
3.05	57.16	28.95
3.10	-	32.98
3.19	-	39.02
3.50	-	-

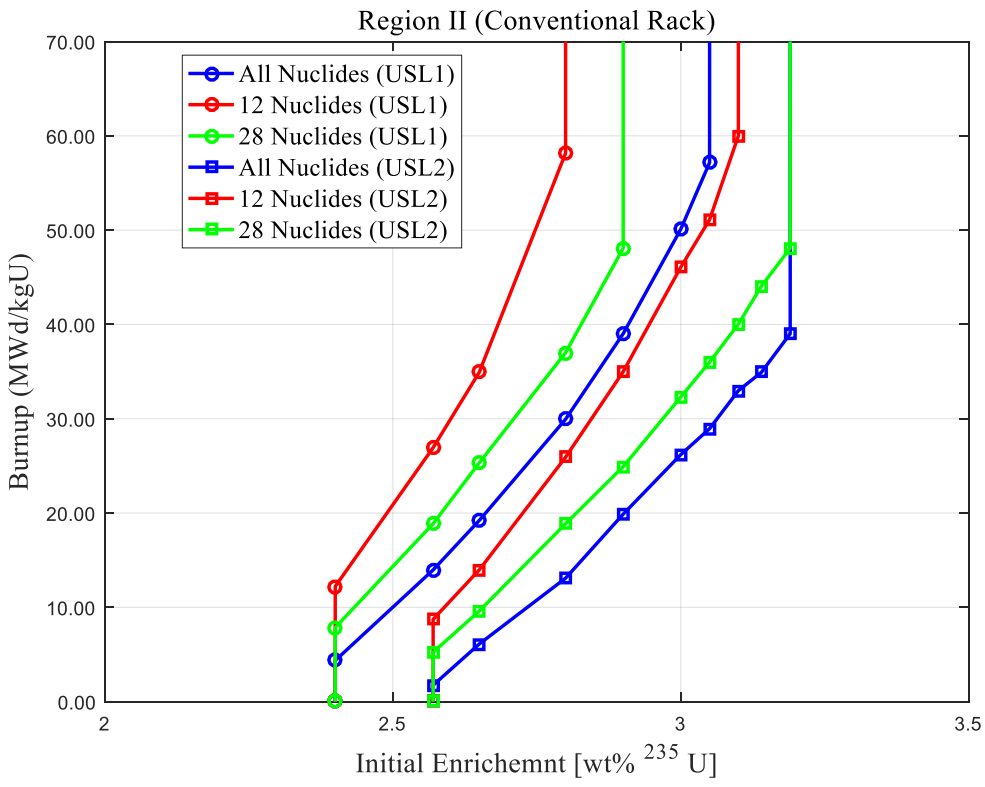


Figure 8. Loading curve for conventional rack.

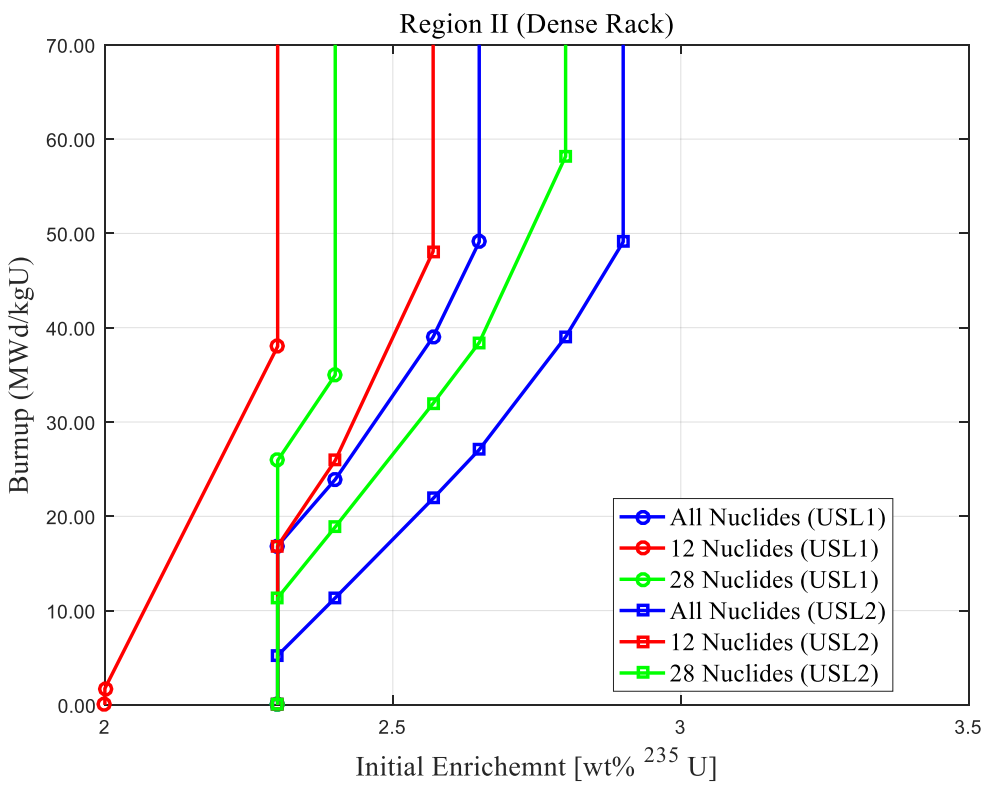


Figure 9. Loading curve for proposed dense rack.

V. Sensitivity Analysis

The main part of this sensitivity analysis is to perform the criticality calculations of racks for the regions I and II. The k_{eff} is calculated while varying three parameters: thickness, material, and composition of the annular cylinder type of neutron absorber. This evaluates the criticality change according to the change of the parameters. The goal of this sensitivity analysis is to find the optimum geometry of racks for the regions I and II to satisfy the criticality regulatory requirements. The criticality of optimized rack geometry is required to meet the reference k_{eff} value of the existing conventional design with the minimum amount of the neutron absorber. Another condition of the optimum geometry is to minimize the rack volume by reducing the pitch of rack, in order to store more spent fuel assemblies than the existing rack design.

5.1. Calculation information

The sensitivity analysis on the regions I and II are performed using the MCS computer code utilizing the ENDF/B-VII.1 continuous energy cross section libraries. Monte Carlo simulations used 10 active, 10 inactive cycles with 20 multicycles, and 100,000 neutrons per cycle. The k_{eff} uncertainties are from 13 to 16 pcm.

5.2. Region I

5.2.1. Absorber thickness

To determine the optimum geometry of the proposed design of the high density spent fuel storage rack in the region I, the variations of neutron multiplication factors with respect to the neutron absorber thickness change are presented in the Figure 10. The radius of water hole that used for placing the guide or instrumentation tube during reactor operation is 1.1430 cm, which is the maximum thickness of the neutron absorber possible.

For the region I, both conventional plate type and annular cylinder type of neutron absorber are used together. The influence on the neutron multiplication factor according to the variation of the thickness of neutron absorber was studied only for the annular cylinder type of neutron absorber with a fixed thickness of the plate neutron absorber. The k_{eff} shows tendency to decrease with increasing the thickness of neutron absorber, and shows the multiplication factor value of 0.64009 for a thickness of 0.823 cm. It is confirmed that the neutron multiplication factor is maintained at a similar level at a thickness exceeding the above range. From these results, the optimum neutron absorber thickness was

selected to be 0.823 cm, considering the requirement of using the minimum amount of the neutron absorber.

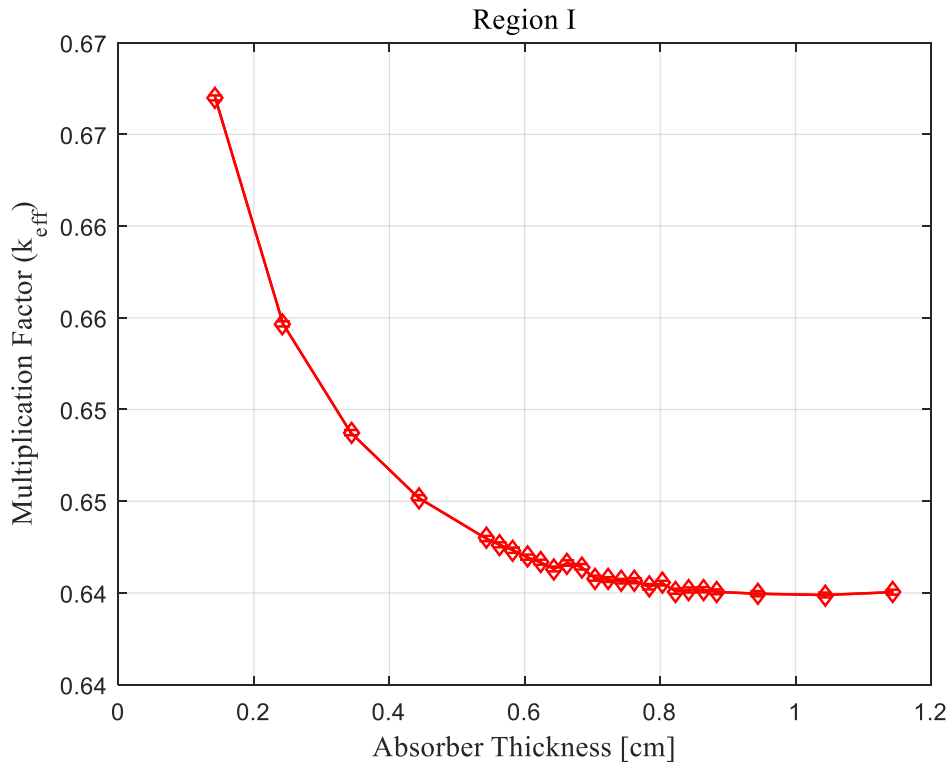


Figure 10. Neutron multiplication factor as function of thickness of annular cylinder type of neutron absorber for region I

5.2.2. Absorber material and concentration

Figure 13 shows the multiplication factor as a function of the boron and gadolinium neutron absorber material concentrations. Through the results of Figure 13, the neutron absorption capacity of boron and gadolinium are compared. The results show that when the gadolinium is used as the neutron absorber, the neutron multiplication factor is lower when the same enrichment is compared below 15.0 at%. The ^{10}B nuclide has lower reaction cross section than the ^{157}Gd nuclide in the thermal region, but the reaction cross section of ^{10}B is larger in the fast region. Therefore, when the concentration of the neutron absorber material is sufficiently high as shown in Figure 13, the amount of neutron absorption of ^{10}B is higher than that of ^{157}Gd . Figure 11 shows the ^{10}B and ^{157}Gd neutron absorption reaction cross sections. This can be confirmed that the use of gadolinium is effective in lowering the neutron multiplication factor when using gadolinium rather than boron when using a low concentration absorber material in terms of efficiency. From this result, the optimum concentration of gadolinium was selected to be 2.0 at%.

Based on 2.0 at% gadolinium, the performance of four neutron absorber material candidates [22-24] was analyzed. The neutron absorber material was selected as ^{10}B , ^{167}Er , ^{151}Eu , ^{149}Sm according to the information of the neutron absorption cross section in Figure 12. As shown in Figure 14, the Gd and Eu neutron absorber material are the most effective in decreasing the neutron multiplication factor.

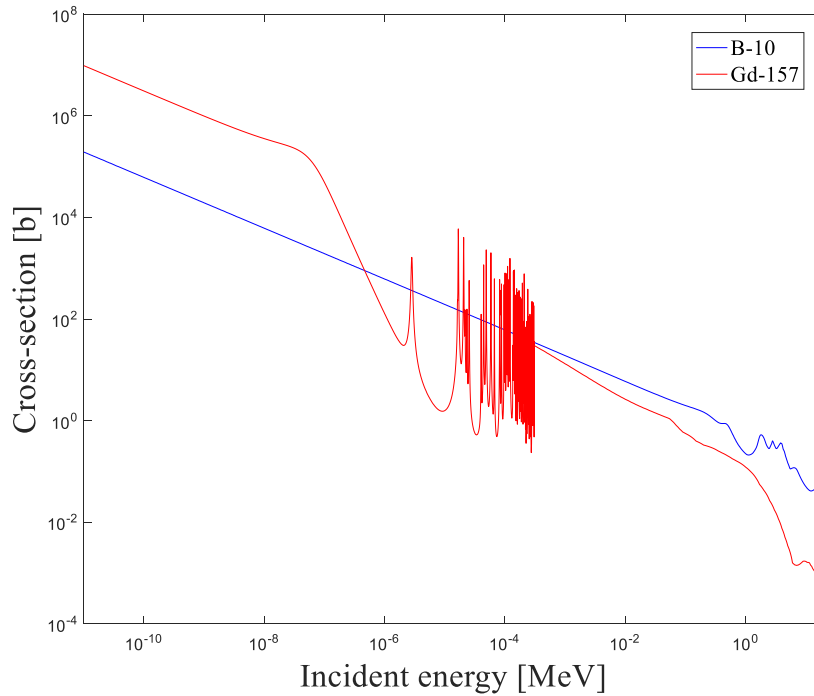


Figure 11. Neutron absorption cross section of ^{10}B and ^{157}Gd as neutron absorber material.

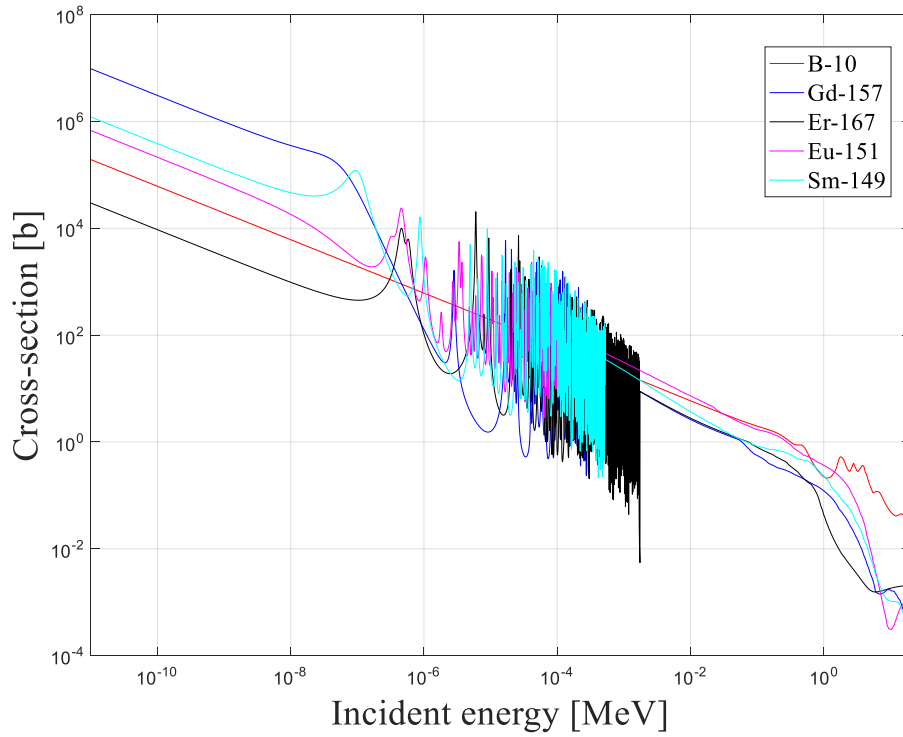


Figure 12. Neutron absorption cross section of selected candidates for neutron absorber material.

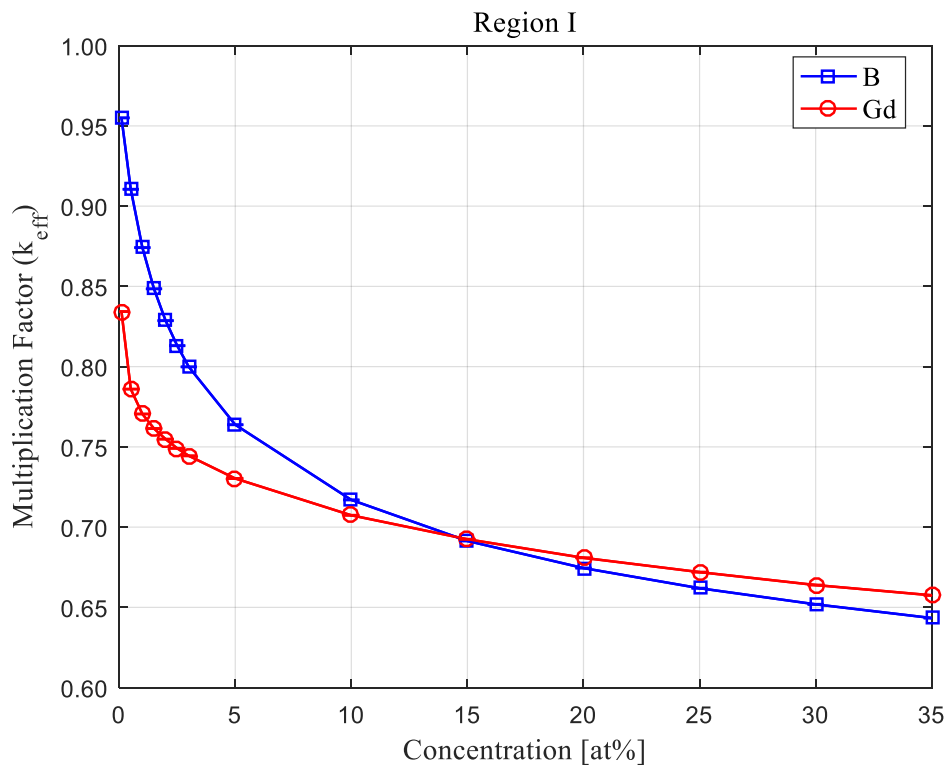


Figure 13. Neutron multiplication factor as function of neutron absorber concentration of boron and gadolinium for region I

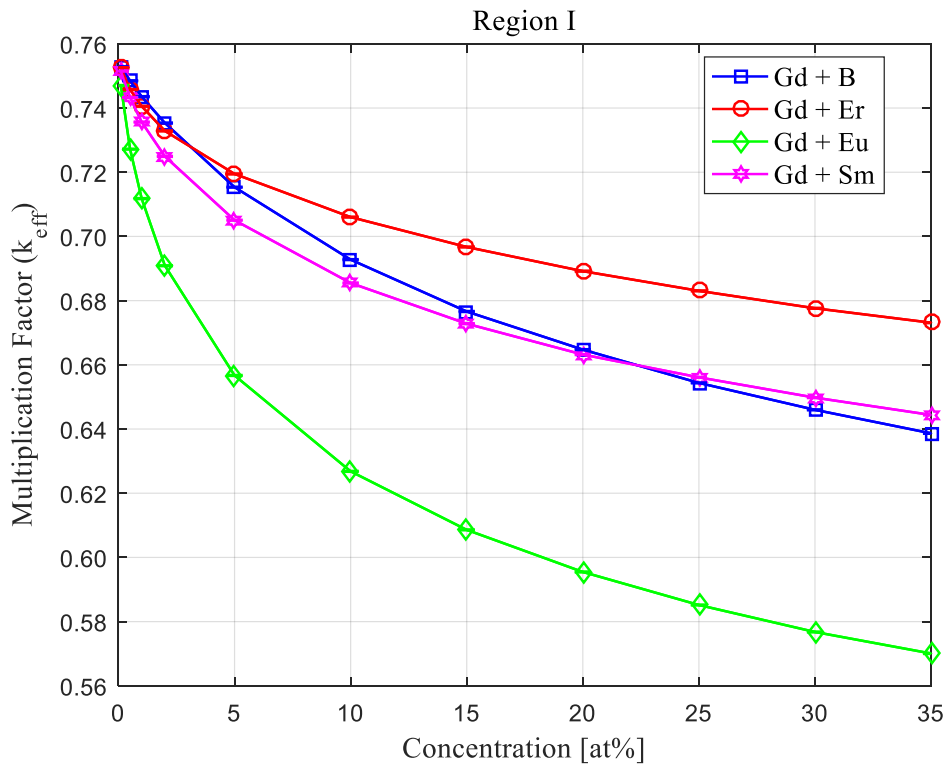


Figure 14. Neutron multiplication factor as function of concentration of neutron absorber material candidates for region I

5.2.3. Rack Pitch

Figure 15 shows the multiplication factor as a function of the rack pitch of region I with selected optimum neutron absorber thickness. The neutron multiplication factor shows tendency to increase continuously as the rack pitch of region I is decreased. The criticality analysis is performed on the models with a rack pitch from 22.60 cm to 27.00 cm of region I conventional geometry. With a composition of Gd 2.0 + Eu 4.5 at%, the k_{eff} value shows 0.85487, which is less than the k_{eff} value of 0.85525 of the conventional design and formed a dense rack with a lower pitch, 23.00 cm.

5.3. Region II

5.3.1. Absorber thickness

The conventional neutron absorber consists of single plate between the assemblies, which increases the rack pitch. The shape of the neutron absorber presented in this study has an annular cylinder shape, that can be inserted into the guide tube position. The spent fuel storage facilities must be maintained in a subcritical state, and thus the neutron multiplication factor should be lower than that

of conventional design. Figure 16 shows the behavior of the neutron multiplication factor with respect to the change in the thickness of the neutron absorber in the annular cylinder. According to the results, the thickness of 0.603 cm maintains the lowest neutron multiplication factor value of 0.97631.

As the thickness of the neutron absorber increases, the amount of neutron absorber increases. However, the k_{eff} is not proportional to the change in the thickness of the neutron absorber. As shown in Figure 16, the multiplication factor is decreased to neutron thickness of about 0.6 cm. From the neutron thickness of about 0.6 cm, the multiplication factor increases as the thickness increases. This phenomenon can be explained by the correlation between the neutron absorber thickness and the flux trap. The flux trap can be decreased by increasing the neutron absorber thickness, since moderation of the fast neutrons is decreased due to the reduced the quantity of water as moderator.

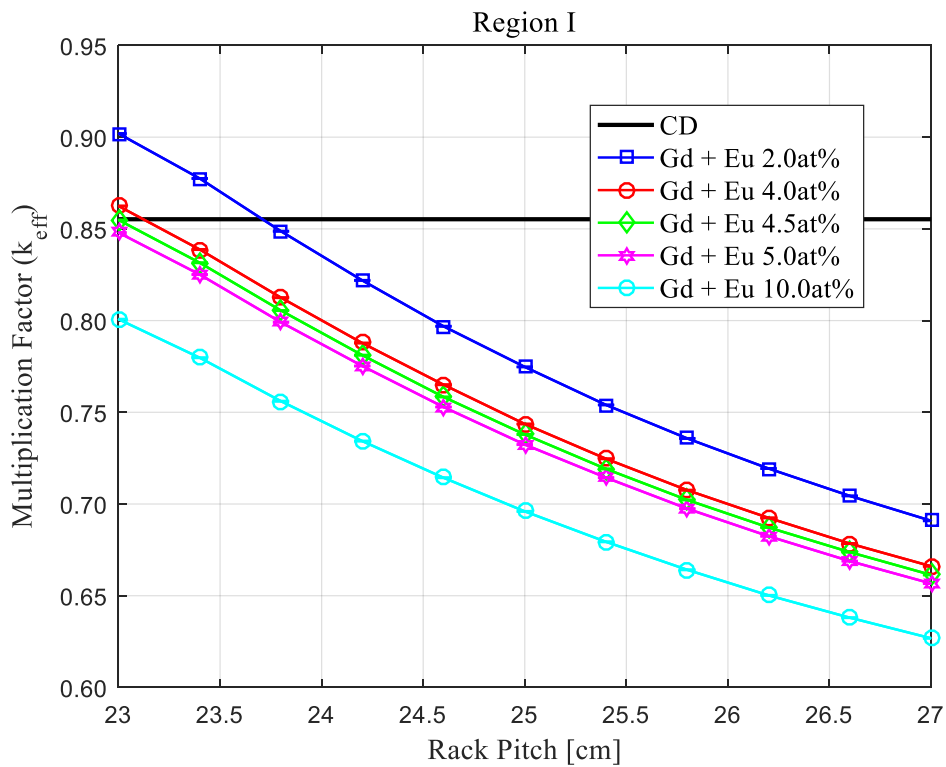


Figure 15. Neutron multiplication factor as function of rack pitch for region I

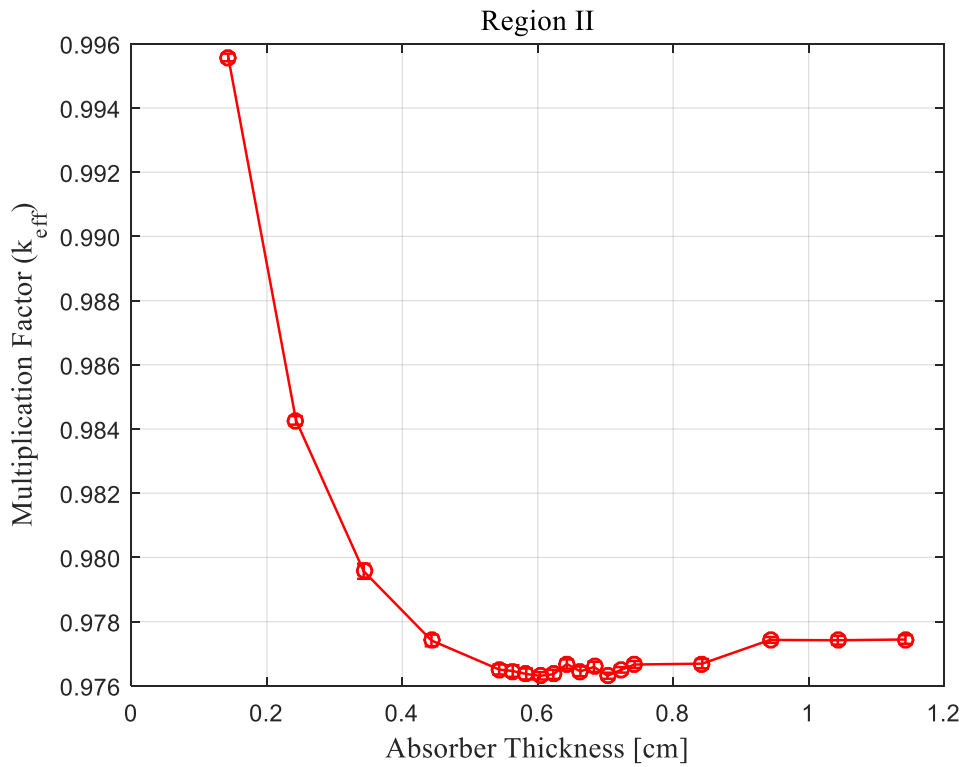


Figure 16. Neutron multiplication factor as function of thickness of annular cylinder type of neutron absorber for region II

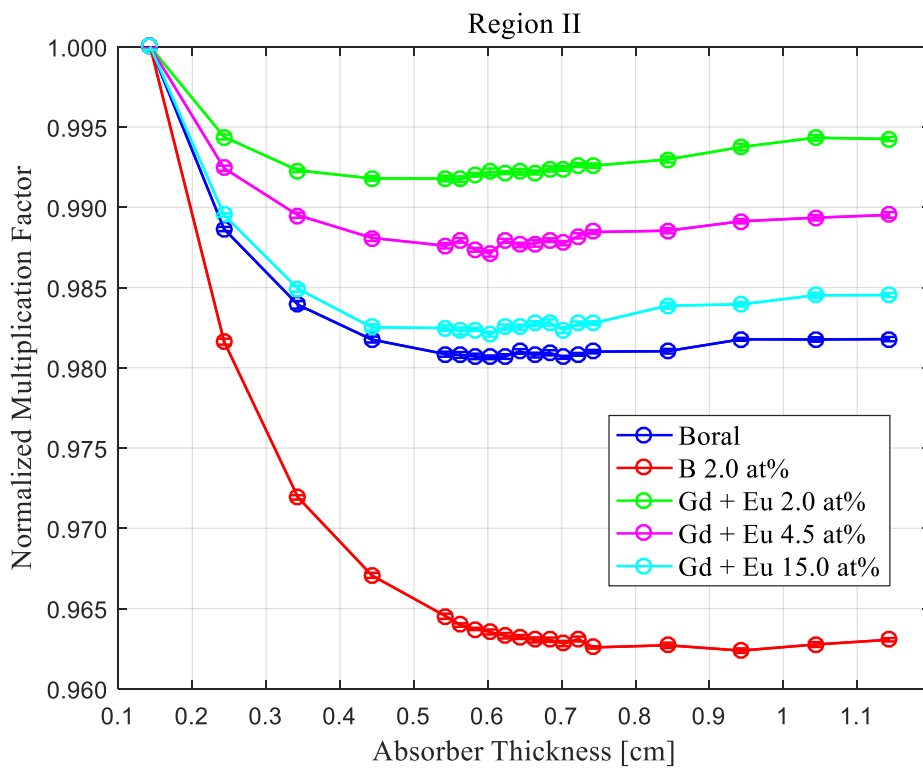


Figure 17. Normalized neutron multiplication factor as function of thickness of neutron absorber

Figures 18-20 show the neutron spectra for the regions of guide tube inserted with annular type of neutron absorber. The regions are divided to four sub-regions associated with the material type: outer water, cladding, absorber, and inner water. The lowest k_{eff} value is obtained when the neutron absorber thickness is 0.603 cm, and the cases with the neutron absorber having a thickness above this value tends to increase the k_{eff} value. When the neutron passes through the guide tube zone filled with absorber, it is thermalized in the outer water region, and the thermal neutrons are absorbed by the neutron absorber material. In the inner water region, the neutrons are once again thermalized and absorbed as they leave the guide tube region. In Figure 20, when comparing between the 0.603 cm and 0.843cm thickness of neutron absorber, the latter volume of the inner water region is less than that of the former. This decreases the amount of neutron absorbed and leads to the k_{eff} value increases.

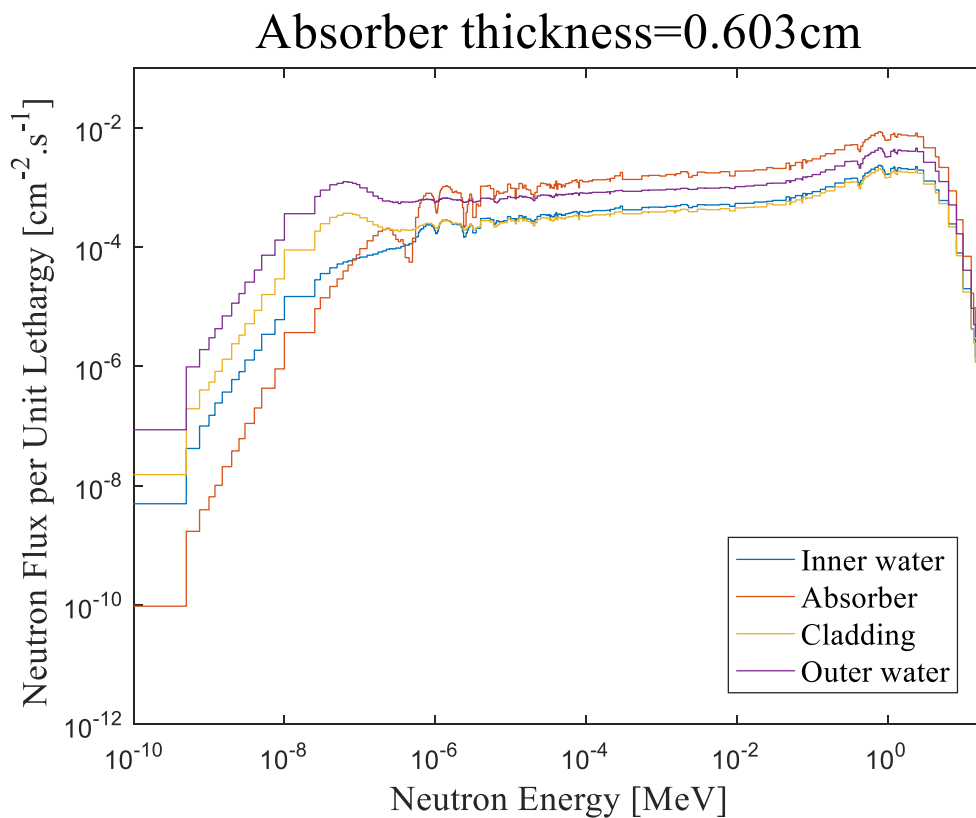


Figure 18. Neutron spectrum of guide tube region (thickness of neutron absorber =0.603cm).

Absorber thickness=0.843cm

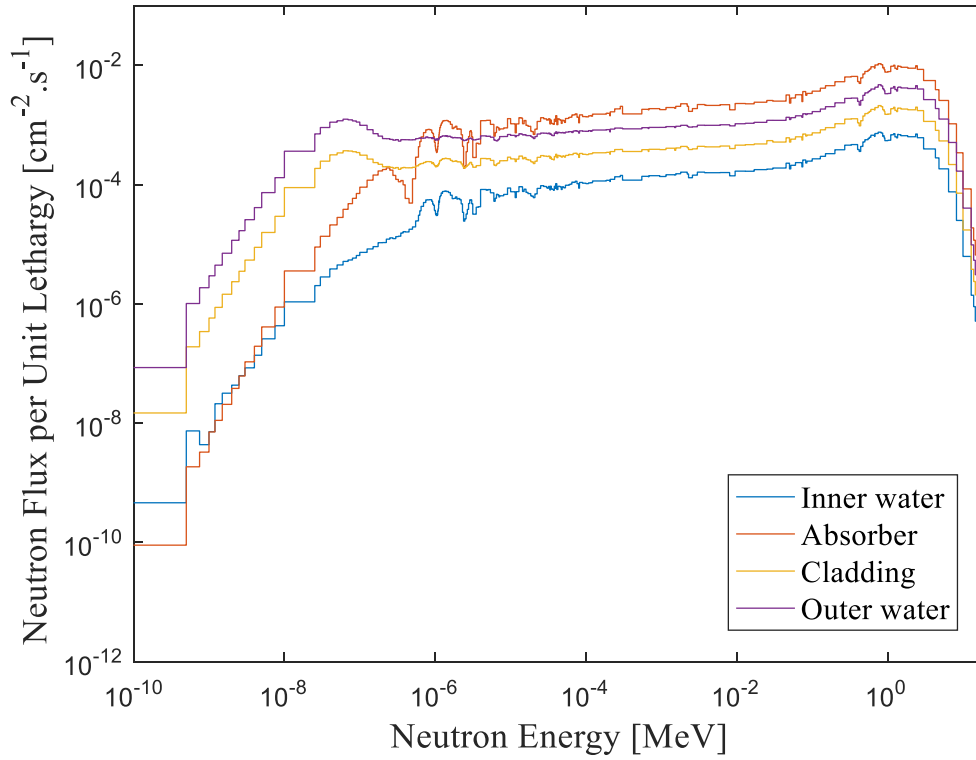


Figure 19. Neutron spectrum of guide tube region (thickness of neutron absorber =0.843cm).

Inner Water Region

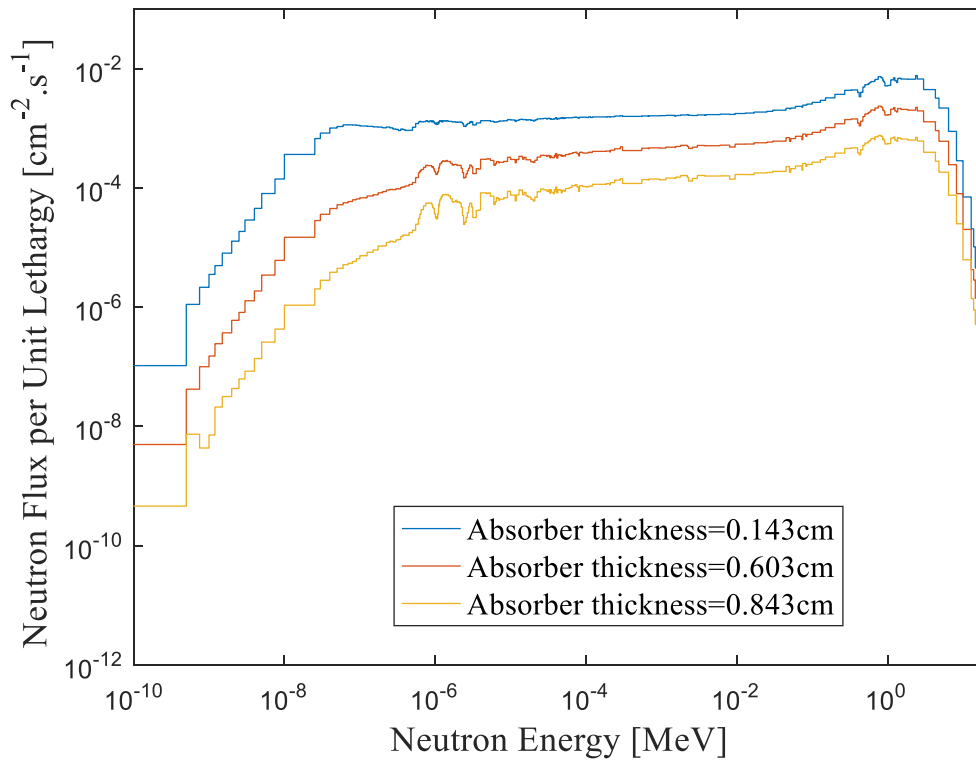


Figure 20. Neutron spectrum of inner water region at guide tube.

5.3.2. Absorber material and concentration

The most commonly used neutron absorber materials are gadolinium and boron, since both isotope has high neutron absorption cross section. ^{157}Gd isotope has about 60 times higher neutron absorption cross section compared to ^{10}B . The gadolinium is the base material for neutron absorber, the other candidates are ^{10}B , ^{167}Er , ^{151}Eu , and ^{149}Sm due to their high thermal neutron absorption cross sections. Figure 12 shows the neutron absorption cross sections for the absorber material candidates.

The neutron multiplication factor is calculated with applying the various material types and concentrations. The additional absorber material to gadolinium compensates the neutron absorption in the energy region, where ^{157}Gd has low neutron absorption cross section. According to the result of Figure 14, this is effective way in reducing the multiplication factor. Among the candidate materials tested, ^{167}Er shows a good performance as an effective material for annular cylinder type neutron absorber.

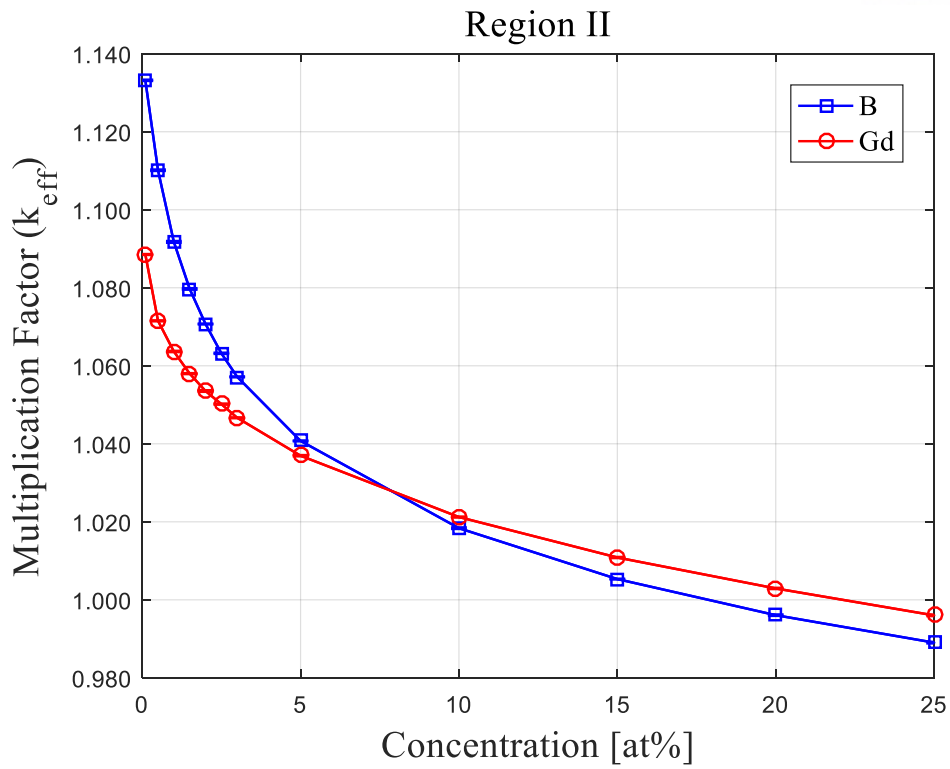


Figure 21. Neutron multiplication factor as function of neutron absorber concentration of boron and gadolinium for region II

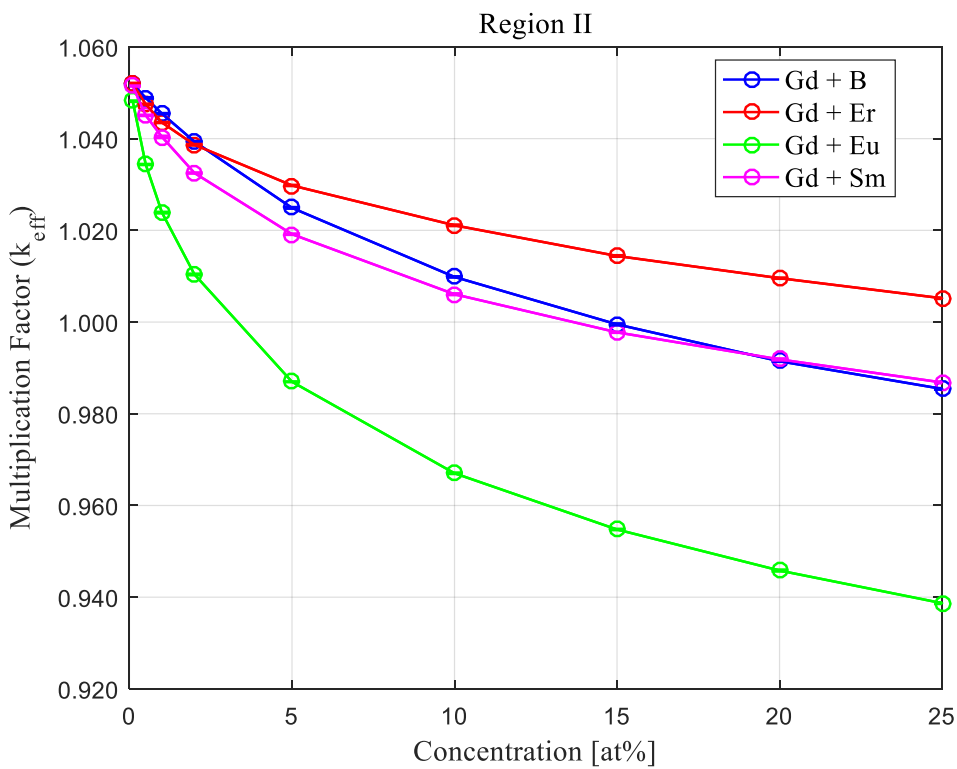


Figure 22. Neutron multiplication factor as function of concentration of neutron absorber material candidates for region II

5.3.3. Rack Pitch

Figure 23 illustrates the multiplication factor behavior as a function of the rack pitch for region II with selected optimum neutron absorber thickness. The rack pitch of region II storage cell can be reduced using an annular cylinder type neutron absorber and a neutron absorber composed of Gd and Eu. The space for plate type neutron absorber and water gap are eliminated, and this lead to the high density spent fuel storage rack. The rack pitch is reduced from 22.60 cm to 21.10 cm, under the condition that the neutron multiplication factor is lower than that of conventional design. The optimum concentration of neutron absorber that meets this criterion is Gd 2.0 and Eu 4.5 atomic percent.

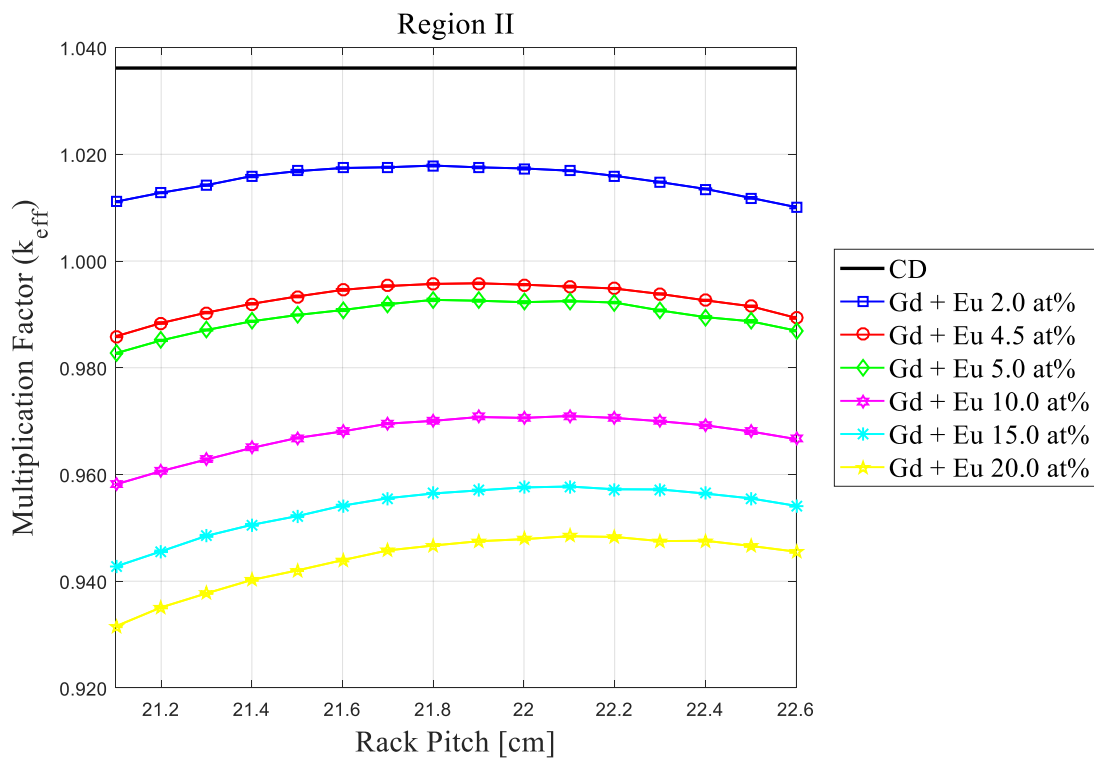


Figure 23. Neutron multiplication factor as function of rack pitch for region II.

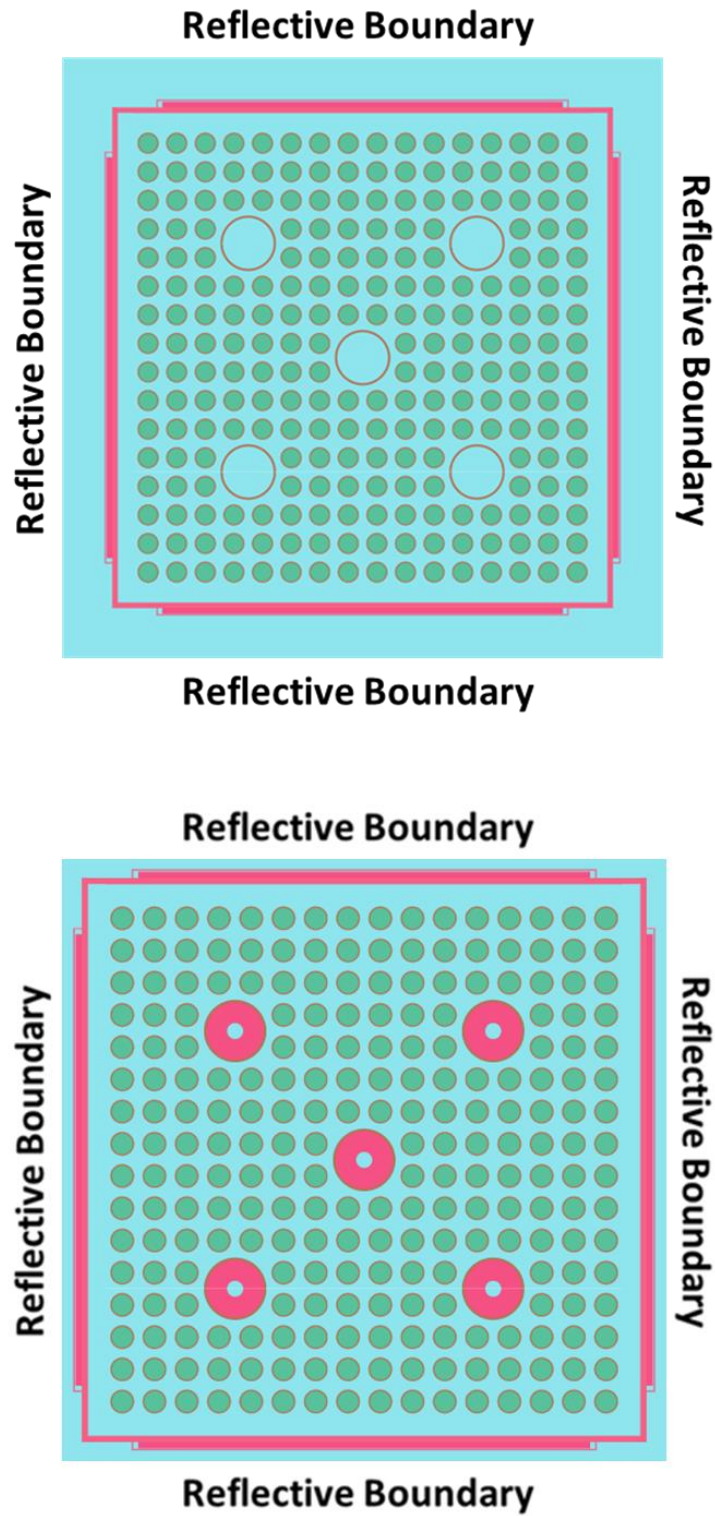


Figure 24. Conventional (Above) and proposed (Below) design of region I.

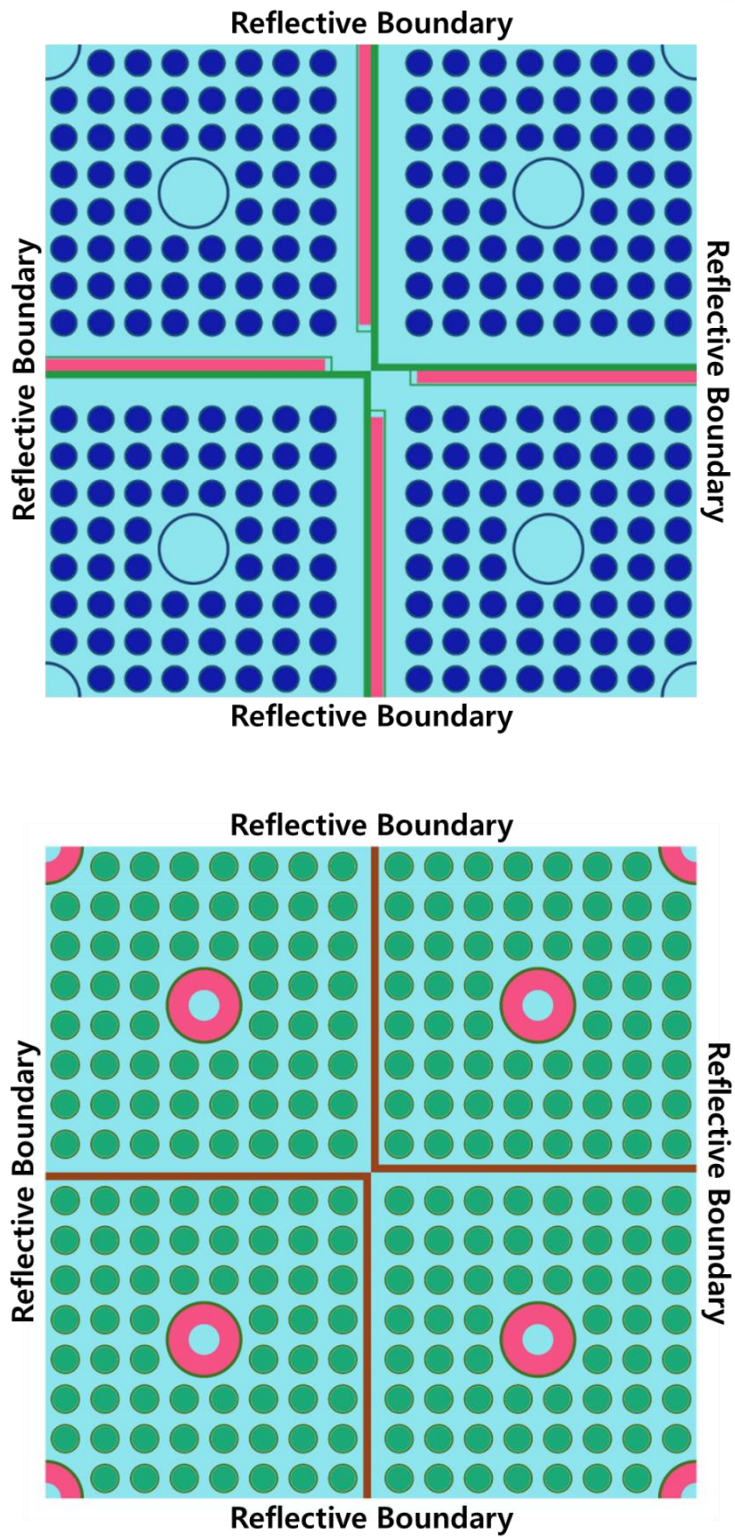


Figure 25. Conventional (Above) and proposed (Below) design of region II.

VI. Conclusion

In the thesis, the research on a design to achieve a high density spent fuel storage rack and the minimum burnup level to satisfy the criticality safety requirement is conducted. As the rack pitch of the storage cell is reduced, the neutron multiplication factor is increased and a strategy to control this increased reactivity has been introduced. The first point is to apply the burnup credit of the nuclear fuel assembly stored in the spent fuel storage, and the other strategy is to insert the neutron absorber in the form of annular cylinder into a guide tube filled with water. For region I, both the conventional plate-type neutron absorber and the proposed annular cylinder-type neutron absorber are used, and the neutron absorber material composition with Gd 2.0 and Eu 4.5 atomic percent is applied to reduce the rack pitch from 27.00 cm to 23.00 cm. In the case of the region II, the annular cylinder type of neutron absorber is introduced to eliminate the plate neutron absorber and reduce the water gap between the fuel assemblies. When the burnup credit is applied based on the nuclear fuel assembly with 3.14 wt% initial enrichment, the multiplication factor decreases by 8099 pcm. As the result, the rack pitch is reduced from 22.60 cm to 21.10 cm with meeting the lower criticality level than that of conventional design of region II spent fuel pool. Also, it was studied which burnup level can satisfy the subcritical condition for each fuel assembly with different initial enrichment under the condition that the critical safety limit value is less than USL1 and USL2. When the conventional rack design is applied on the fuel assembly has selected 17 different initial enrichment, the fuel assemblies with an initial concentration of 3.10 or higher did not meet the critical safety standards, and when a dense rack was used, the fuel assemblies with an initial concentration of 3.50 or higher could not be stored to region II. As a result, we expect to increase storage capacity by 24.7% and 14.7% in regions I and II, respectively, when the proposed dense rack is applied. The given approach provides the additional 30 and 624 spent fuel assemblies vacancies in regions I and II, respectively, for the Shin Kori 5,6 units, which can store 112 fuel assembly in region I storage and 4246 fuel assemblies in region II.

References

1. Kelleher and David S., “Public Participation in the Siting of Nuclear Waste Facilities: International Lessons and the Korean Experience,” *Korea Observer*, vol.48, no.2, pp. 277-323, 2017.
2. J. C. Wagner, “Computational Benchmark for Estimation of Reactivity Margin from Fission Products and Minor Actinides in PWR Burnup Credit,” NUREG/CR-6747, ORNL/TM-2001/306, U.S. Nuclear Regulatory Commission, Oak Ridge National Laboratory, Oct. 2001.
3. J.C. Wagner, “Assessment of Reactivity Margins and Loading Curves for PWR Burnup-Credit Cask Designs,” NUREG/CR-6800, ORNL/TM-2002/6, prepared for the U.S. Nuclear Regulatory Commission by Oak Ridge National Laboratory, Oak Ridge, Tennessee, Mar. 2003.
4. I. C. Gauld, “Strategies for Application of Isotopic Uncertainties in Burnup Credit,” NUREG/CR-6811, ORNL/TM-2001/257, prepared for the U.S. Nuclear Regulatory Commission by Oak Ridge National Laboratory, Oak Ridge, Tennessee, Jun. 2003.
5. D.E. Mueller, “Evaluation of the French Haut Taux de Combustion (HTC) Critical Experiment Data,” NUREG/CR-6979. ORNL/TM-2007/083, prepared for the U.S. Nuclear Regulatory Commission by Oak Ridge National Laboratory, Oak Ridge, Tennessee, Sep. 2008.
6. I. C. Gauld, “Uncertainties in Predicted Isotopic Compositions for High Burnup PWR Spent Nuclear Fuel,” NUREG/CR-7012, ORNL/TM-2010/41, prepared for the U.S. Nuclear Regulatory Commission by Oak Ridge National Laboratory, Oak Ridge, Tennessee, Jan. 2011.
7. G. Radulescu, “An Approach for Validating Actinide and Fission Product Burnup Credit Criticality Safety Analyses—Isotopic Composition Predictions,” NUREG/CR-7108. ORNL/TM-2011/509, prepared for the U.S. Nuclear Regulatory Commission by Oak Ridge National Laboratory, Oak Ridge, Tennessee, Apr. 2012.
8. J. M. Scaglione, “An Approach for Validating Actinide and Fission Product Burnup Credit Criticality Safety Analyses—Criticality (k_{eff}) Predictions,” NUREG/CR-7109, ORNL/TM-2011/514, prepared for the U.S. Nuclear Regulatory Commission by Oak Ridge National Laboratory, Oak Ridge, Tennessee, Apr. 2012.
9. R.F. Mahmoud, M.K. Shaat, M.E. Nagy, S.A. Agamy, A.A. Abdelrahman, “Burn-up credit in criticality safety of PWR spent fuel,” *Nuclear Engineering and Design*, 280: 628-633. 2014.
10. “MCNP6 User’s Manual. U.S.: Los Alamos National Laboratory”, LA-CP-13-000634 Version 1.0., 2013.
11. H. Lee, C. Kong, D. Lee, “Status of Monte Carlo Code Development at UNIST,” PHYSOR-2014, Kyoto, Japan, Sep. 28-Oct. 3. 2014.
12. Chadwick M.B., “ENDF/B-VII.1 Nuclear Data for Science and Technology: Cross Sections, Covariances, Fission Product Yields and Decay Data,” Nucl. Data. Sheet. 112:2887-2996, 2011.

13. Horelik, N., Herman, B., "MIT benchmark for evaluation and validation of reactor simulations (BEAVRS)," Version 1.1.1. MIT: MIT Computational Reactor Physics Group, 2013.
14. Hoogenboom, J.E., Martin, W.R., Petrovic, B., "Monte Carlo performance benchmark for detailed power density calculation in a full-size reactor core," Benchmark Specifications Revision 1.1., 2010.
15. Na, B.C., "Benchmark on the VENUS-2 MOX Core Measurements," NEA/NSC/DOC (2000)7, 2000.
16. U.S. NRC, "Recommendations for Addressing Axial Burnup in PWR Burnup Credit Analyses," 2013.
17. U.S. NRC, "10 CFR 70.24 Criticality Accident Requirements".
18. J. Jang, W. Kim, S. Jeong, E. Jeong, J. Park, M. Lemaire, H. Lee, Y. Jo, P. Zhang, D. Lee, "Validation of UNIST Monte Carlo Code MCS for Criticality Safety Analysis of PWR Spent Fuel Pool and Storage Cask," *Annals of Nuclear Energy*, 114: 495-509, 2018.
19. S. Jeong, J. Jang, W. Kim, A. Khassenov, D. Lee, "Evaluation of NUREG/CR-6361 and NUREG/CR-6698 Methodologies of PWR Spent Fuel Pool and Storage Cask," KNS Spring Meeting, Jeju, Korea, May. 17-19. 2017.
20. J. C. Dean and R. W. Tayloe, Jr., "Guide for Validation of Nuclear Criticality Safety Computational Methodology," NUREG/CR-6698, prepared for the U.S. Nuclear Regulatory Commission by Oak Ridge National Laboratory, Oak Ridge, Tennessee, Jan. 2001.
21. "International Handbook of Evaluated Criticality Safety Benchmark Experiments," NEA/NCS/DOC(95)03/IV. 2014
22. M. Kim, H. Lee, J. Jong, D. Sohn, "사용후핵연료 저장 수조에서의 흡수체 물질별 핵적 성능 분석," KRS Autumn Meeting, Yeosu, Korea, Oct. 10-17. 2014.
23. M. Kim, H. Lee, D. Sohn, "첨단흡수소재를 이용한 사용후핵연료 저장 수조에서의 핵적 성능 분석," KNS Spring Meeting, Jeju, Korea, May. 6-8. 2015.
24. M. Kim, H. Lee, D. Sohn, "The effectiveness of Gd contents of fuel basket wall in UNF shipping & storage cask," Waste Management, Phoenix, AZ, USA, Mar 6-10. 2016.

Acknowledgements

가장 먼저, 연구의 흥미를 일깨워 주시고 많은 지도와 가르침을 주신 이덕중 교수님께 감사드립니다. 진로 고민을 하였던 학부 졸업학기에 교수님께서 주신 기회로 대학원 진학을 결정하게 되었고 석사과정 동안 교수님의 도움과 격려 그리고 충고가 있어 이렇게 무사히 석사 졸업을 하게 되었습니다. 그동안 국내뿐만 아니라 해외에서도 인턴으로 근무하며 많은 경험을 할 수 있었고, 교수님의 지도를 받고 따르며 공학도로서 더욱 성장할 수 있었습니다. 아직 부족한 점이 많아 앞으로도 교수님의 말씀을 따르고 기억하며 더욱 발전할 수 있도록 노력하겠습니다.

저의 석사 논문을 심사해주시고 많은 조언을 해주신 이현철 교수님과 윤의성 교수님께 감사드립니다. 격려와 함께 많은 질문을 해주시고 논점을 제시하여 주셔서 저의 논문이 한층 더 발전할 수 있었습니다.

연구실의 많은 동료분들에게 감사의 말씀드립니다. Zhang Peng 박사님, Jiankai 박사님, Matthieu 박사님, Alexey 박사님, 태우형, 현석이형, 원경, azamat, 치동, 한주, 진수, 윤기, 수영, 지원, 은, 재림, 기호, 용민, 옹희, Bamidele, Khang, Tung, Dos, Tuan, Nhan, Lezani 곁에서 함께 열심히 해주시고 관심을 가져주셔서 감사합니다. 연구뿐만 아니라 많은 것들을 함께 할 수 있어 그 시간이 정말 즐거웠습니다.

항상 믿고 응원해주시고 부족함 없이 지원해주신 부모님과 곁에서 힘이 되어준 형에게 감사드립니다. 그리고 어릴 때부터 사랑으로 키워주시고 언제나 반갑게 맞아주시는 할머니, 할아버지께도 감사드립니다. 지금껏 받은 사랑에 보답하는 아들, 동생, 손자가 되겠습니다.